NKG2D-Dependent Antitumor Effects of Chemotherapy and Radiotherapy against Glioblastoma

Weiss, Tobias; Schneider, Hannah; Silginer, Manuela; Steinle, Alexander; Pruschy, Martin; Polić, Bojan; Weller, Michael; Roth, Patrick

Source / Izvornik: **Clinical Cancer Research, 2018, 24, 882 - 895**

Journal article, Accepted version
Rad u časopisu, Završna verzija rukopisa prihvaćena za objavljivanje (postprint)

https://doi.org/10.1158/1078-0432.CCR-17-1766

Permanent link / Trajna poveznica: https://urn.nsk.hr/urn:nbn:hr:184:482828

Weiss, Tobias; Schneider, Hannah; Silginer, Manuela; Steinle, Alexander; Pruschy, Martin N; Polic, Bojan; Weller, Michael; Roth, Patrick (2018). *NKG2D-dependent anti-tumor effects of chemotherapy and radiotherapy against glioblastoma.* Clinical Cancer Research, 24(4):882-895

DOI: 10.1158/1078-0432.CCR-17-1766

http://clincancerres.aacrjournals.org/lookup/doi/10.1158/1078-0432.CCR-17-1766

NKG2D-dependent anti-tumor effects of chemotherapy and radiotherapy against glioblastoma

Tobias Weiss[1], Hannah Schneider[1], Manuela Silginer[1], Alexander Steinle[2], Martin Pruschy[3], Bojan Polić[4], Michael Weller[1], Patrick Roth[1]

[1]Department of Neurology and Brain Tumor Center, University Hospital Zurich and University of Zurich, Switzerland; [2]Institute for Molecular Medicine, University of Frankfurt, Germany; [3]Department of Radiation Oncology, University Hospital Zurich and University of Zurich, Switzerland; [4] Department of Histology & Embryology, Faculty of Medicine, University of Rijeka, Croatia

Corresponding author: Dr. Patrick Roth, Department of Neurology, University Hospital Zurich, Frauenklinikstrasse 26, 8091 Zurich, Switzerland, Tel.: +41 (0)44 255 5511, Fax: +41 (0)44 255 4380, E-mail: patrick.roth@usz.ch

Conflict of interest: The authors declare no potential conflicts of interest.

Running title: NKG2D-dependent anti-glioma effects of chemoradiotherapy

Keywords: glioblastoma, NKG2D, temozolomide, irradiation, immunotherapy

Funding: This study was supported by grants from the Gertrud-Hagmann Foundation and the Swiss Cancer League (KFS-3478-08-2014) to PR and “Hochspezialisierte Medizin Zurich” (HSM-2) to MW and PR.

Statement of translational relevance:

Temozolomide and radiotherapy are the adjuvant standard of care for patients with glioblastoma. This manuscript demonstrates an unprecedented role of the NKG2D-dependent immune pathway for the efficacy of these anti-cancer therapies against glioblastoma. Both treatment modalities induce immune-stimulatory NKG2D ligands also in unfavorable but clinically relevant settings of MGMT overexpression, TMZ resistance and at tumor recurrence. This promotes the role of the NKG2D system as an attractive immunotherapeutic target in glioblastoma at primary diagnosis and at recurrence. Furthermore, it provides a strong rationale for future combination studies of conventional radiochemotherapy and NKG2D-based immunotherapy.

Abstract

Purpose: NKG2D is a potent activating immune cell receptor and glioma cells express the cognate ligands (NKG2DL). These ligands are inducible by cellular stress and temozolomide (TMZ) or irradiation (IR), the standard treatment of glioblastoma, could affect their expression. However, a role of NKG2DL for the efficacy of TMZ and IR has never been addressed.

Experimental Design: We assessed the effect of TMZ and IR on NKG2DL *in vitro* and *in vivo* in a variety of murine and human glioblastoma models including glioma-initiating cells and a cohort of paired glioblastoma samples from patients before and after therapy. Functional effects were studied with immune cell assays. The relevance of the NKG2D system for the efficacy of TMZ and IR was assessed *in vivo* in syngeneic orthotopic glioblastoma models with blocking antibodies and NKG2D knockout mice.

Results: TMZ or IR induced NKG2DL *in vitro* and *in vivo* in all glioblastoma models and glioblastoma patient samples had increased levels of NKG2DL after therapy with TMZ and IR. This enhanced the immunogenicity of glioma cells in a NGK2D-dependent manner, was independent from cytotoxic or growth inhibitory effects, attenuated by O^6-methylguanine-DNA-methyltransferase (MGMT) and required the DNA damage response. The survival benefit afforded by TMZ or IR relied on an intact NKG2D system and was decreased upon inhibition of the NKG2D pathway.

Conclusion: The immune system may influence the activity of convential cancer treatments with particular importance of the NKG2D pathway in glioblastoma. Our data provide a rationale to combine NKG2D-based immunotherapies with TMZ and IR.

Introduction

Glioblastoma is the most common malignant primary brain tumor in adults with a dismal prognosis (1). The first-line treatment in patients below 70 years of age includes surgical resection as feasible, radiotherapy and concomitant and maintenance chemotherapy with temozolomide (TMZ), an alkylating agent that induces DNA damage (2, 3). In addition to these treatment modalities, several promising immunotherapeutic approaches against glioblastoma are currently being evaluated (4, 5). These efforts are supported by the observation that glioma cells express molecules that allow for an interaction with cells of the immune system such as major histocompatibility complex (MHC) class I and class II molecules (6) as well as MHC class I-like ligands which bind to the activating immune cell receptor natural-killer group 2 member D (NKG2D) (7). In humans, NKG2D ligands (NKG2DL) comprise the MHC class I-related chains (MIC) A and B (MICA, MICB) and the UL16 binding proteins (ULBP) 1–6 (8). These ligands are expressed on human glioma cells *in vitro (9)* and *in vivo* (10) as well as on glioma-initiating cells (GIC), a subpopulation of cells with stem cell properties (11, 12). In mice, NKG2DL comprise the retinoic acid early inducible-1 (RAE-1) proteins, members of the H60 family (H60a, H60b, H60c) and the murine UL16-binding protein like transcript-1 (MULT-1) which are also expressed by mouse glioma cells (9, 13). All NKG2DL bind to the NKG2D receptor which is one of the major activating receptors on natural killer (NK) cells (8). In addition to NK cells, this receptor is constitutively expressed on NKT cells, αβ CD8 T cells and γδ T cells (8, 14). Furthermore, its expression is induced on CD4 T cells by tumor necrosis factor (TNF)-α and interleukin (IL)-15 (15, 16). However, various glioma-derived humoral and cellular immunosuppressive mechanisms preclude an efficient anti-tumor immune response, including the expression of transforming growth factor (TGF)-β (17), prostaglandin E2 (PGE2) (18), IL-10 (19), growth and differentiation

factor (GDF)-15 (20), lectin-like transcript 1 (LLT1) (21), indoleamine 2,3-dioxygenase (IDO) (22), programmed death ligand 1 (PD-L1) (23), as well as the presence of immunosuppressive regulatory T cells (Tregs) (24) and M2-polarized microglia (25). Enhancing the immunogenicity of glioma cells may be achieved either by inhibition of these immunosuppressive mechanisms (26) or by promoting immune activating signals such as the NKG2DL (27). Since various cellular stress stimuli including malignant transformation of cells or DNA damage can induce NKG2DL (8), we explored whether TMZ or irradiation (IR) as part of the standard treatment for glioblastoma increase NKG2DL levels on glioma cells and whether this promotes their immunogenicity. We also defined the molecular mechanisms underlying the TMZ- and IR-induced NKG2DL expression in glioma cells. Finally, we investigated the significance of the NKG2D system for the survival benefit gained with TMZ and IR in several immunocompetent mouse glioma models.

Material and Methods

Cells and materials

The human glioma cell lines LN-18 and LN-229 were kindly provided by Dr. N. de Tribolet (Centre Hospitalier Universitaire Vaudois, Lausanne, Switzerland). LN-229-R cells were generated by repetitive exposure to TMZ resulting in a shift of the EC_{50} (28). Generation of LNT-229_MGMT and LNT-229_neo (29) and LN-18_shMGMT and LN-18_puro cells (30) has been described. SMA-560 glioma cells were obtained from Dr. D. Bigner (Duke University Medical Center, Durham, North Carolina, USA) and GL-261 were obtained from the National Cancer Institute (Frederick, Maryland, USA). SMA-560_Turbo650 and GL-261_NirFP were created by lentiviral transduction of GL-261 and SMA-560 cells with plasmids encoding near-infrared fluorescent proteins Turbo650 and NirFP (Evrogen, Moscow, Russia) and selection by fluorescence-activated cell sorting (FACS). Adherent cell lines were maintained in Dulbecco's Modified Eagle Medium (DMEM, Invitrogen, Basel, Switzerland), containing 2 mM L-glutamine (Gibco Life Technologies, Paisley, UK), and 10% fetal calf serum (FCS, Biochrom KG, Zug, Switzerland). The GIC cell lines S-24 and ZH-305 were generated from human glioblastoma patient specimens (31). After tumor removal, tissue was dissociated using a papain system (Worthington, New Jersey, USA) and a gentleMACS™ Dissociator (Miltenyi Biotec, Bergisch Gladbach, Germany). These cells were then maintained as suspension cultures in Neurobasal Medium with B-27 supplement (20 µl/ml) and Glutamax (10 µl/ml) from Invitrogen and fibroblast growth factor (FGF)-2, epidermal growth factor (EGF) (20 ng/ml each; Peprotech, Rocky Hill, Pennsylvania, USA) and heparin (32 IE/ml; Ratiopharm, Ulm, Germany). All cell lines were routinely tested for Mycoplasma using PCR (last test in december 2016). For all experiments described herein, the adherent cells were allowed to attach over a 24 h period. Subsequently, the

experiments were carried out in serum-free medium. KU-60019 (Selleckchem, Houston, Texas, USA) is a potent and specific ataxia-telangiectasia mutated (ATM) inhibitor, concentrations < 1.5 µM ensure specificity for ATM. TMZ, kindly provided by Schering-Plough (Kenilworth, New Jersey, USA), was prepared in stock solutions (100 mM) in dimethylsulfoxide (DMSO). N-(2-chloroethyl)-N'-cyclohexyl-N-nitrosourea (CCNU) was kindly provided by Medac (Wedel, Germany). Cells were irradiated using a cobalt-60 source (Sulzer, Winterthur, Switzerland) and for different fractionations the approximative biological effective dose and dose per fraction according to the linear quadratic model (32) were determined using the R package 'DVHmetrics' (https://cran.r-project.org/web/packages/DVHmetrics/index.html) under the assumption of an α/β ratio of 10 for human glioma cell lines. Thiazolyl blue tetrazolium bromide (MTT) was obtained from AxonLAb (Baden, Switzerland).

Antibodies and flow cytometry

The following monoclonal antibodies (mAbs) were used for the assessment of cell surface expression of MICA, MICB, ULBP2, ULBP3, RAE-1, MULT-1, H60 or blocking of NKG2D: MICA (AMO1, mouse IgG1), MICB (BMO1, mouse IgG1), ULBP2 (BUMO1, mouse IgG1), ULBP3 (CUMO3, mouse IgG1). Their generation has been described (33). RAE-1_FITC and MULT-1_PE and blocking anti-human NKG2D (clone 149810) were obtained from R&D Systems Europe (Abingdon, UK). H60_PerCP was obtained from Novus Biologicals (Littleton, Colorado, USA). Blocking but not depleting anti-mouse NKG2D (clone C7) was obtained from eBioscience (San Diego, California, USA). As controls, we used isotype-matched antibodies from Sigma-Aldrich (Steinheim, Germany). The PE-conjugated goat anti-mouse IgG from Dako (Baar, Switzerland) was used as secondary antibody where appropriate. Cells were detached with Accutase

(Life technologies), preincubated in phosphate-buffered saline (PBS) with 2% FCS, and stained with specific mAbs (10 µg/ml) or matched mouse Ig isotype for 30 min on ice, followed by incubation with PE-conjugated secondary antibody for 30 min where appropriate. After washing, flow cytometric analyses were performed using a BD FACSVerse Analyzer (BD, Allschwil, Switzerland). In case of intracellular staining for $ATM^{ser1981}$ Fix/Perm Buffer Set from BioLegend (San Diego, California, USA) was used. For flow cytometric assessment of tumor-infiltrating lymphocytes, live/dead staining with FVS 510, anti-CD3_ PerCP-Cy5.5, anti-CD4_FITC, anti-CD8_APC-H7, anti-NKp46_PE, anti-IFN-γ_APC and anti-TCRγ/δ_ BV421 from BioLegend (San Diego, California, USA) was used. Specific fluorescence indexes (SFI) were calculated by dividing median fluorescence obtained with the specific antibody by median fluorescence obtained with isotype control antibody. For *in vivo* experiments fluorescence intensity was expressed as median fluorescence intensity. Data was analyzed with FlowJo software (Tree Star, Stanford, California, USA).

Immune cell cytotoxicity assay

We used a flow cytometry-based cytotoxicity assay to determine immune-mediated glioma cell lysis (34). Specific lysis was expressed as percentage of cell death of the $PKH\text{-}26^{+}$ labeled targets. Percentage of target cell lysis was corrected for spontaneous background lysis by subtracting the percentage of dead cells in control samples (targets alone) from the percentage of dead cells within the test samples. As effector cells, we used either splenocytes isolated from mice, human NK cells isolated from PBMC by negative selection using NK cell isolation kit (Miltenyi Biotec, Bergisch Gladbach, Germany) or NKL cells obtained from M.J. Robertson (Indiana University School of

Medicine, Indianapolis, Indiana, USA). For blocking experiments, NKL cells were preincubated for 2 h at 4°C with anti-NKG2D or IgG1 isotype control, and the antibody was also present during the co-incubation of target and effector cells. All experiments were done in triplicates.

Real-time PCR

Total RNA was isolated using the NucleoSpin RNA II system from Macherey-Nagel (Düren, Germany) and cDNA was prepared using the iScript cDNA Synthesis Kit from Bio-Rad Laboratories AG (Cressier, France). For real-time PCR, gene expression was measured in an ABI Prism 7000 Sequence Detection System (Applied Biosystems, Foster City, California, USA) with SYBR Green Master Mix (Thermo Fisher Scientific (Waltham, Massachusetts, USA) and primers (Microsynth AG, Balgach Switzerland) at optimized concentrations. Primers for MICA, MICB, ULBP2 and ULBP3 have been published (35). Primers used to detect murine NKG2DL were RAE-1 forward 5′-TTTGGGAGCACAACCACAGAT-3′, reverse 5′-TAAAGTTGGCGGGCTGAAAGA-3′, MULT-1 forward 5′-CTGCCAGTAACAAGGTCCTTTC-3′, reverse 5′-GCTGTTCCTATGAGCACCAATG-3′, H60a forward 5′-CTGAGCTATCTGGGGACCATAC-3′, and reverse 5′-AGTCTTTCCATTCACTGAGCAC-3′. As reference gene, we used human HPRT1: forward 5′-TGAGGATTTGGAAAGGGTGT-3′, reverse 5′-GAGCACACAGAGGGCTACAA-3′ and mouse HPRT1: forward 5′- TTGCTGACCTGCTGGATTAC-3′, reverse 5′-TTTATGTCCCCCGTTGACTG-3′ respectively. The conditions were 40 cycles at 95°C/15 s and 60°C/1 min. Standard curves were generated for each gene. Relative quantification of gene expression was determined by comparison of threshold values.

All results were normalized to HPRT1 and calculated with the ΔCTT method for relative quantification.

Determination of cytotoxicity, acute cytostatic or clonogenic effects

For determination of cytotoxicity, 5×10^3 cells were seeded per well in 96-well plates, allowed to attach for 24 h (adherent cells) and irradiated or exposed to TMZ, CCNU or staurosporine as indicated for 72 h in serum-free medium. Percentage of living cells was determined by flow cytometry after live/dead staining with Zombie Aqua™ Fixable Viability Kit (BioLegend, San Diego, California, USA). For acute growth inhibition assays, we used the same experimental setting but either crystal violet staining (for adherent cells) or MTT (for suspension cells) as read-out. Clonogenic survival assays were performed by seeding 10^2 cells per well in 96-well plates. After 24 h, the cells were irradiated or exposed to TMZ, CCNU, or staurosporine as indicated for 24 h in serum-free medium, followed by observation for 20 days. As read-out methods, we used again either crystal violet staining or MTT.

Immunoblot analyses

For the detection of proteins in cell lysates, cells were lysed and processed as previously described (28). Thirty µg of protein were used per lane and visualization of protein bands was accomplished using horseradish peroxidase (HRP)-coupled secondary antibodies (Sigma-Aldrich) and enhanced chemiluminescence (Pierce/Thermo Fisher, Madison, Wisconsin, USA).

Immunofluorescence

Cells were cultured in chamber slides with polystyrene-treated glass (BD Biosciences), fixed with 4% paraformaldehyde and permeabilized with 0.5% Triton X-100 (Sigma-Aldrich). Blocking with 3% FCS was followed by incubation with anti-ATM protein kinase pS1981 monoclonal antibody (Rockland, Gilbertsville, Pennsylvania, USA) (diluted 1:100) overnight at 4°C. Donkey anti-mouse IgG Alexa Fluor 488-labeled secondary antibody (Life technologies, Carlsbad, California, USA) was used at 1:200. Slides were mounted in Vectashield Mounting Media with DAPI (Burlingame, California, USA) and images were acquired by using a Leica TCS SP5 confocal microscope.

Mice and animal experiments

All experiments were done in accordance with the guidelines of the Swiss federal law on animal protection and they were approved by the cantonal veterinary office. C57BL/6 mice were purchased from Charles River Laboratories (Sulzfeld, Germany). VM/Dk mice were bred in pathogen-free facilities at the University of Zurich. NKG2D$^{-/-}$ mice have been previously described (36) and were kindly provided by D. H. Busch (Munich, Germany). Mice of 6 to 12 weeks of age were used in all experiments in groups of 7-10 mice. For intracranial tumor implantation SMA-560 cells (5×10^3) or GL-261 cells (2×10^4) were stereotactically implanted into the right striatum at day 0. Mice were observed daily and sacrificed as indicated or in the survival experiments when developing neurologic symptoms. If indicated, local cranial radiotherapy with a single dose of 12 Gy was performed at day 10 after tumor implantation using a Gulmay 200 kV X-ray unit at 1 Gy/min at room temperature. If indicated, mice received TMZ (10 mg/kg/day) per oral gavage from day 7-11 after tumor implantation. MRI was performed with a 4.7 T small animal magnetic resonance imager (Pharmascan; Bruker Biospin, Ettlingen, Germany)

at day 13 after tumor implantation. Coronal T2-weighted images were acquired using Paravision 6.0 (Bruker BioSpin). Mean +/- SD of the tumor volume in mm^3 from 5 mice/group were determined by the formula (length x width x depth)/2.

For *in vivo* blockade of NKG2D signaling, mice were injected i.p. with 100 ug of the blocking but not depleting anti-NKG2D antibody (clone C7) (37) or with isotype control in PBS. Antibodies were given either one day before and one day after tumor implantation or at day 6 and 7 after tumor implantation and were re-injected every 7 days until the mice were sacrificed. Time of antibody administration is indicated in the figure legends.

Isolation of orthotopic tumor cells was performed on day twelve after tumor implantation. Brains were harvested after transcardial perfusion with ice-cold PBS to remove all circulating leukocytes from the CNS. Tumor cells were separated from myelin and red blood cells using a Percoll gradient suspension (Sigma-Aldrich). Cells were washed with PBS and stained with Zombie Aqua™ Fixable Viability Kit and fluoro-conjugated antibodies specific to indicated cell surface markers for flow cytometry.

Tissue microarray of patient samples

Studies were approved by the Institutional Review Board (KEK-StV-Nr.19/08) and informed consent was received prior to inclusion to the study. Twenty-one pairs of primary (before chemoradiation) and recurrent glioblastoma (variable timepoints after chemoradiation) specimens from patients who underwent brain tumor resection between 2000 and 2014 at the Department of Neurosurgery, University Hospital Zurich (Zurich, Switzerland) were collected. Immunohistochemistry was performed as described (31) using anti-MICA, anti-MICB, anti-ULBP2, or anti-ULBP3 antibodies from Sino Biological (Lucerna-Chem AG, Luzern, Switzerland) or anti-programmed death-

ligand 1 (PD-L1) from Cell Signaling Technology (Danvers, Massachusetts, USA). Images were analyzed in an unsupervised and blinded fashion using TMARKER, a software toolkit for histopathological staining estimation (38).

Statistical analysis

Data are presented as means +/- SD. Experiments were repeated at least three times, if not indicated differently. Viability and acute and clonogenic cell growth studies were performed at least in triplicates. Statistical analyses were performed in GraphPad Prism (La Jolla, CA, USA) using multiple two-tailed Student's t-tests and correction for multiple comparisons using the Holm-Sidak method. For analysis of tissue microarray data, we used Wilcoxon matched-pairs signed rank test. For analysis of heterogeneity of immunohistochemically stained NKG2DL, we calculated the intraclass correlation coefficient (ICC) (39) as a statistical measure to assess staining variation for 2 tissue cores from each tumor sample by using the R-package 'ICC' (https://cran.r-project.org/web/packages/ICC/index.html). Kaplan Meier survival analysis was performed to assess survival differences among the treatment groups and p values were calculated with Gehan-Breslow-Wilcoxon test. Throughout all figures, significance was concluded at *$p < 0.05$ and **$p < 0.01$.

Results

TMZ induces NKG2DL expression in glioma cells independent from cytotoxic and growth inhibitory effects

Exposure of glioma cells to TMZ has growth inhibitory as well as cytotoxic effects. To define the sensitivity of LN-18 and LN-229 cells to TMZ, we treated these cells with a broad range of TMZ concentrations and determined cell death, acute growth inhibition and clonogenic cell survival (Fig. 1A). Since NKG2DL are up-regulated in response to various stress stimuli, we explored in a next step whether TMZ induces the expression of NKG2DL in these cells. We observed an induction of several NKG2DL on mRNA and protein cell surface level over a wide concentration range (Fig. 1A, Suppl. Fig 1A-B) including low concentrations with minor cytotoxic and growth inhibitory effects as well as clinically relevant concentrations around plasma levels of 30-80 μM of TMZ that are achieved in human patients (40). To evaluate the effect on other activating immune cell receptor ligand systems, we assessed CD112 and CD155 as ligands of the human DNAX accessory molecule-1 (DNAM-1, CD226) activating immune cell receptor. In contrast to NKG2DL, the cell surface expression of CD112 and CD155 was unaffected by TMZ (Suppl. Fig. 1C). Next, we examined the effect of TMZ on NKG2DL expression in GIC, a subpopulation of glioma cells with stem-like properties which are associated with resistance to chemotherapy and irradiation (41). S-24 cells were relatively resistant to TMZ with an EC_{50} value of 267 μM in clonogenic survival assays whereas ZH-305 cells were more sensitive with an EC_{50} of 7.3 μM (Fig. 1B). TMZ induced several NKG2DL on mRNA and cell surface protein levels in both GIC lines. Again, there was no induction of DNAM-1 ligands (Suppl. Fig. 1D). Furthermore, we determined the expression of NKG2DL on mouse glioma cells and their induction by TMZ. GL-261 and

SMA-560 cells differed in their sensitivity to TMZ. The EC_{50} for clonogenic cell survival was ≈ 50 µM for GL-261 and >500 µM for SMA-560 (Fig. 1C). Similar to human cells, exposure to TMZ resulted in an up-regulation of NKG2DL in both murine glioma cell models. H60a is not expressed in C57BL/6 mice and the syngeneic GL-261 cells (42) and was therefore not detected in this cell line.

To corroborate our findings that the upregulation of NKG2DL is not a general response pattern of glioma cells to cell death induction but rather a specific response to alkylating chemotherapy, we exposed LN-18 and LN-229 cells to different concentrations of staurosporine. Despite its strong effect on glioma cell viability, none of the NKG2DL was up-regulated by staurosporine (Suppl. Fig. 1E). However, CCNU, another alkylating agent commonly used in patients with recurrent glioblastoma (43) also induced NKG2DL already at low concentrations, close to those typically achieved in the plasma of patients (3.4-3.8 µM) (44) (Suppl. Fig. 1F).

Irradiation induces NKG2DL in human and mouse glioma cells independent from cytotoxic and cytostatic effects

Since radiotherapy belongs to the standard of care for glioma patients, we also assessed the effect of IR on NKG2DL expression in different glioma models. LN-18 cells were more sensitive to irradiation than LN-229 cells with an EC_{50} value of 4 Gy vs. 11 Gy in clonogenic survival assays. In both cell lines, IR induced the expression of several NKG2DL mRNA and cell surface protein (Fig. 2A). The induction of NKG2DL cell surface expression following IR was also confirmed when different fractionation schemes were applied (Suppl. Fig. 2A). Consistent with the TMZ data, there was no induction of DNAM-1 ligands upon irradiation (Suppl. Fig. 2B). In S-24 and ZH-305 GIC, irradiation had minor cytotoxic effects with an EC_{50} value of > 20 Gy but clear effects on

clonogenic survival with EC_{50} values ≈ 5 Gy. A clinically relevant single fraction in the range of 2-4 Gy increased NKG2DL mRNA and cell surface protein levels (Fig. 2B). We also confirmed the irradiation-mediated induction of NKG2DL in GL-261 and SMA-560 mouse glioma cells. In both cell lines, irradiation upregulated NKG2DL on mRNA as well as on cell surface protein level (Fig. 2C).

TMZ- but not irradiation-mediated NKG2DL induction is modulated by MGMT and both depend on ATM signaling

MGMT promoter methylation predicts benefit from alkylating chemotherapy with TMZ in glioblastoma. To explore whether the TMZ-mediated induction of NKG2DL is influenced by MGMT, we used sub-cell lines of LN-18 with a stably silenced *MGMT* gene (30) or LNT-229 cells that stably overexpress *MGMT* (29). The modulation of *MGMT* expression affected the sensitivity to TMZ (Fig. 3A), but not to IR (Suppl. Fig. 3A). Furthermore, *MGMT* expression significantly decreased TMZ-mediated NKG2DL induction. This was demonstrated by an increased NKG2DL induction upon shRNA-mediated *MGMT* silencing in LN-18 glioma cells that naturally express *MGMT* and a diminished NKG2DL induction in *MGMT*-overexpressing LNT-229 cells compared to *MGMT*-deficient wild-type LN-229 cells (Fig. 3B). The IR-mediated upregulation of NKG2DL was unaffected by the MGMT status (Suppl. Fig. 3B). Glioma cells can also acquire resistance to TMZ independent from MGMT expression. Mechanistically, this is linked, amongst others, to the down-regulation of DNA mismatch-repair proteins (28). Because this acquired resistance is a challenge in clinical practice that needs alternative treatment options, we assessed the induction of potentially immune-activating NKG2DL in a glioma cell line with acquired TMZ resistance (28). Also in these

cells, TMZ or IR induced the cell surface protein level of NKG2DL. The same effect was observed after IR (Suppl. Fig. 3C, D).

To elucidate the molecular mechanisms mediating the treatment-induced NKG2DL induction in glioma cells, we assessed the ATM pathway as part of the DNA damage response to genotoxic stress induced by TMZ (45). In LN-229 and S-24 cells, we detected an increase of active phospho-ATM^{Ser1981} upon exposure to TMZ (Fig. 3C). Inhibition of ATM using RNA interference (Suppl. Fig. 3E) or KU-60019, a specific ATM inhibitor that inhibited ATM at 1.25 µM with little toxicity (Suppl. Fig. 3F), abrogated the TMZ-induced up-regulation of MICA and MICB in LN-229, S-24 cells (Fig. 3D). We confirmed this also for ZH-305 cells (Suppl. Fig. 3G). Furthermore, we observed this ATM-dependency also for irradiation-mediated NKG2DL induction (Fig. 3D, Suppl. Fig. 3G).

Exposure to TMZ and IR promote glioma cell immunogenicity in a NKG2D-dependent manner

To investigate functional effects of the TMZ- or RT-induced NKG2DL induction, we performed cytotoxicity assays using polyclonal human NK cells or NKL cells (46) as immune effectors. Pre-exposure of LN-229 or S-24 cells to TMZ resulted in an enhanced immune cell-mediated cytolysis (Fig. 4A, Suppl. Fig. 4A). In contrast, exposure of *MGMT*-overexpressing LNT-229 cells to TMZ at the same concentrations did not enhance immune-cell mediated cytolysis (Suppl. Fig. 4B). Pre-incubation of effector cells with blocking but not depleting anti-NKG2D antibodies abrogated the TMZ-induced glioma cell susceptibility to immune cell killing (Fig. 4A). Similarly, LN-229 or S-24 cells that were pre-irradiated with 2 Gy were more susceptible to immune cell-mediated cytolysis in a NKG2D-dependent manner (Fig. 4B).

NKG2DL levels are increased in vivo in syngeneic glioma models following treatment with TMZ or IR as well as in human glioblastoma following radiochemotherapy

To study the effect of TMZ and irradiation on glioma-associated NKG2DL *in vivo*, we generated GL-261_niRP and SMA-560_TurboFP650 mouse glioma cells, which stably express near-infrared fluorescent proteins and which are syngeneic to C57BL/6 or VM/Dk mice. This allowed for the detection of these cells by flow cytometry (Fig. 5A) and the specific assessment of NKG2DL protein levels on the cell surface *ex vivo*. After orthotopic tumor cell injection, we treated mice either with a single dose of local IR at day 10 or with TMZ per oral gavage for 5 consecutive days starting at day 7 after tumor cell inoculation. At day 12, mice were euthanized and the tumors explanted. TMZ and irradiation led to an up-regulation of NKG2DL in both orthotopic murine glioma cell models with a more pronounced effect in the SMA-560 model (Fig. 5A).

To study the effect of chemo- and radiotherapy on glioma-associated NKG2DL in human glioblastoma patients, we created a tissue microarray (TMA) encompassing 21 paired formalin-fixed samples of human glioblastoma specimens obtained before and after treatment with TMZ and/or radiotherapy. From 9 of these paired samples, we could also isolate RNA. Compared to basal expression, we detected increased levels of several NKG2DL on mRNA as well as on cell surface protein level after treatment with TMZ or IR or both (Fig. 5B). Based on 2 cores from each tumor, we found a heterogeneous expression of NKG2DL within tumors, particularly for ULBP2 and ULBP3 (Suppl. Fig. 5A). We did not observe correlations between NKG2DL and survival or NKG2DL and the immunosuppressive ligand PD-L1 in this small patient population.

There were also no significant differences in PD-L1 expression between primary and recurrent human glioblastoma samples (Suppl. Fig. 5B-D).

The NKG2D system contributes to the therapeutic effects of TMZ and irradiation in glioma

Finally, we asked whether the NKG2D system plays any role for the survival benefit gained from TMZ or irradiation in murine glioma models. We inhibited the NKG2D system in fully immune-competent, orthotopic SMA-560 glioma-bearing mice by repetitive intraperitoneal injections of a blocking but not depleting anti-NKG2D antibody (37). Its biological activity reflecting target inhibition was verified by decreased *ex vivo* cytolysis of SMA-560 cells upon TMZ exposure or irradiation by immune effector cells isolated from anti-NKG2D-treated mice (Suppl. Fig. 6A). At the treatment schedules used, either IR or TMZ prolonged survival, but this effect was more prominent for IR. Administration of the anti-NKG2D antibody abrogated the survival benefit conferred by TMZ and attenuated the IR-mediated survival benefit in SMA-560 glioma-bearing mice (Fig. 6A). This NKG2D-dependent effect of TMZ or IR in SMA-560 glioma-bearing mice was also present when the anti-NKG2D antibody was administered at day 6 and 7 post tumor implantation when tumors had already been established (Suppl. Fig. 6B). To confirm the importance of an intact NKG2D system for the efficacy of TMZ and IR in glioma in a second syngeneic setting, we used NKG2D knockout ($NKG2D^{-/-}$) mice, as an even more robust model. These mice were treated with the same regimen of TMZ or IR. In addition, we also included the combination of both treatments, reflecting the current standard of care for human glioblastoma patients. There was no difference in median survival of glioma-bearing $NKG2D^{-/-}$ or NKG2D-intact mice when no treatment was administered. TMZ or irradiation prolonged the median

survival of GL-261 tumor-bearing mice and the combination of both therapies further increased the survival (Fig. 6B). However, the survival gain conferred by TMZ, irradiation or the combination of both was significantly reduced in NKG2D$^{-/-}$ mice (Fig. 6B). The survival data were corroborated by MRI. At day 6 post tumor implantation we could not clearly delineate the tumor due to superimposing post-surgery alterations, but at day 13 post tumor implantation, we observed reduced activity of the anti-tumor treatments with regard to tumor growth in NKG2D-deficient mice (Fig. 6C, Suppl. Fig. 6C). Finally, we analyzed tumor-infiltrating immune cells. TMZ alone significantly reduced NK and CD4 T cells, and IR as well as the combination of TMZ and IR reduced NK cells within the tumor microenvironment (Fig. 6D). There was no difference in the composition of tumor-infiltrating immune cells in NKG2D$^{-/-}$ *versus* NKG2D-intact mice. However, the activation status of infiltrating immune cells, which did not differ in untreated NKG2D$^{-/-}$ or NKG2D-intact mice, was impaired in NKG2D$^{-/-}$ mice upon treatment. NK cells as well as CD4 and CD8 T cells produced more IFN-γ in NKG2D-intact mice following treatment with TMZ, IR or the combination of TMZ and IR, and this induction was attenuated in NKG2D$^{-/-}$ mice. In NKG2D-intact mice, $\gamma\delta$ T cells produced more IFN-γ upon treatment with TMZ, IR or the combination of TMZ and IR compared to NKG2D$^{-/-}$ mice. In NKG2D$^{-/-}$ mice, we observed more IFN-γ production in $\gamma\delta$ T cells only upon IR (Fig. 6D, Suppl. Fig. 6D-F).

Discussion

TMZ chemotherapy and radiotherapy constitute the standard treatment modalities in patients with newly diagnosed glioblastoma (43). The anti-glioma effects of TMZ and IR comprise different molecular mechanisms such as induction of cell cycle arrest, senescence and apoptosis (47, 48). Furthermore, there is increasing evidence that cell death upon exposure to TMZ or IR can promote anti-tumor immune responses by releasing tumor-associated antigens or damage-associated molecular pattern molecules such as calreticulin, adenosine triphosphate or high-mobility group box 1 protein (49-51). In addition to these soluble and potentially immune-stimulating molecules, glioma cells express membrane-bound ligands to the activating immune cell receptor NKG2D which basically enables target cell killing without prior sensitization and irrespective of MHC restriction.

We observed an up-regulation of several NKG2DL on mRNA and protein level upon exposure to TMZ, CCNU or IR in several mouse and human glioma cells including stem-like cells (Fig. 1 and 2, Suppl. Fig. 1 and 2). NKG2DL induction by TMZ has previously been reported in four other human glioma cell lines (52). We found that the NKG2DL induction was independent from cytotoxic or growth inhibitory effects and was achieved at clinically relevant concentrations of chemotherapeutic agents and low doses of IR. Furthermore, we confirmed the up-regulation of NKG2DL on glioma cells upon treatment with TMZ or IR *in vivo* in two orthotopic mouse glioma models (Fig. 5A). The use of fluorescently labeled glioma cells excluded contaminating signals from immune cells which could also express NKG2DL (53). These findings were further corroborated by an analysis of paired samples of human glioblastoma tissue specimens obtained from patients during initial surgery and at tumor recurrence following radio-

and/or chemotherapy. The increased NKG2DL expression levels after alkylating chemotherapy or radiotherapy support our *in vitro* data as well as findings from the mouse studies (Fig. 5B). Changes in glioma cell NKG2DL levels may be confounded by other factors than treatment such as passenger mutations which occur during the course of the disease (54, 55). Despite these limitations, our data strongly suggest that NKG2DL expression levels are increased following radiochemotherapy. Together with the observation that NKG2DL can also be induced in TMZ-resistant cells (Suppl. Fig. 3C and D), this provides a rationale to investigate NKG2D-targeting therapies (27) also at tumor recurrence.

We demonstrate that the up-regulation of NKG2DL upon TMZ or IR requires ATM (Fig. 3D, Suppl. Fig. 3G) which supports the concept that the DNA damage response is one stimulus for the induction of NKG2DL (56). Consequently, ATM inhibitors may potentially counteract NKG2D-dependent anti-tumor immune effects. This needs to be considered in future trials evaluating the activity of such ATM inhibitors as radiosensitizers (57).

Although the net effect of NKG2D ligand induction is of rather small magnitude, it has important functional consequences. The induction of NKG2DL by TMZ or IR enhanced the immunogenicity of glioma cells including GIC and rendered the cells more susceptible to immune-mediated cytolysis (Fig. 4, Suppl. Fig. 4A). Chemotherapy and radiotherapy have various effects on tumor cells and the microenvironment comprising both immune-stimulatory and immune-suppressive mechanisms. Our study indicates that treatment-associated NKG2DL induction constitutes a relevant immune-stimulatory mechanism because inhibition of NKG2D signaling abrogated the enhanced cytolysis. Furthermore, tumor-infiltrating NK, CD4, CD8 T cells and to some extent also $\gamma\delta$ T cells

produced more IFN-γ in a NKG2D-dependent manner upon treatment with TMZ and/or irradiation (Fig. 6D). This emphasizes the relevance of the NKG2D-mediated immune-stimulatory mechanism of TMZ and IR and adds another relevant mechanism to the concept of immunogenic cell death.

We did not only demonstrate that TMZ- and radiotherapy-mediated NKG2DL induction can be used as a strategy to render glioma cells more immunogenic but also that the full efficacy of TMZ and IR against glioblastoma depends on an intact NKG2D system. The survival benefit gained with these treatment modalities was diminished upon blockade of NKG2D signaling with an inhibitory but non-depleting antibody or in NKG2D knockout mice (Fig. 6A and B, Suppl. Fig. 6A-C). Inhibition or deficiency of NKG2D in mice did not result in a significant survival difference without additional treatment, suggesting that the basal expression levels of NKG2DL are too low to promote a relevant immune response (7, 10, 26, 34, 58).

The NKG2DL induction upon TMZ treatment or IR could provide a rationale for future studies investigating the synergistic application of these conventional treatment modalities with other NKG2D-based immunotherapeutic strategies (27). So far, one phase I study has used pure NK cells for adoptive immunotherapy in patients with recurrent malignant gliomas (59). However, no concomitant treatment with TMZ or IR was administered and additive or synergistic effects to this adoptive cell therapy need to be explored in future clinical trials.

In summary, the present dataset demonstrates the relevance of a so far unrecognized mechanism mediating anti-tumor effects of TMZ and IR that is likely to be clinically relevant. Based on our findings, further studies evaluating the combination of radiochemotherapy with additional NKG2D-based immunotherapeutic strategies should be considered for the treatment of glioblastoma.

References

1. Weller M, Wick W, Aldape KD, Brada M, Berger SM, Nishikawa R, et al. Glioma. Nat Rev Dis Primers. 2015:15017.

2. Stupp R, Mason WP, van den Bent MJ, Weller M, Fisher B, Taphoorn MJB, et al. Radiotherapy plus concomitant and adjuvant temozolomide for glioblastoma. The New England journal of medicine. 2005;352:987–96.

3. Weller M, van den Bent M, Tonn JC, Stupp R, Preusser M, Cohen-Jonathan-Moyal E, et al. European Association for Neuro-Oncology (EANO) guideline on the diagnosis and treatment of adult astrocytic and oligodendroglial gliomas. The lancet oncology. 2017;18:e315-e29.

4. Preusser M, Lim M, Hafler DA, Reardon DA, Sampson JH. Prospects of immune checkpoint modulators in the treatment of glioblastoma. Nature reviews Neurology. 2015;11:504-14.

5. Weiss T, Weller M, Roth P. Immunotherapy for glioblastoma: concepts and challenges. Curr Opin Neurol. 2015.

6. Dutoit V, Herold-Mende C, Hilf N, Schoor O, Beckhove P, Bucher J, et al. Exploiting the glioblastoma peptidome to discover novel tumour-associated antigens for immunotherapy. Brain. 2012;135:1042-54.

7. Crane CA, Han SJ, Barry JJ, Ahn BJ, Lanier LL, Parsa AT. TGF-beta downregulates the activating receptor NKG2D on NK cells and CD8+ T cells in glioma patients. Neuro Oncol. 2010;12:7-13.

8. Raulet DH, Gasser S, Gowen BG, Deng W, Jung H. Regulation of Ligands for the NKG2D Activating Receptor. Annu Rev Immunol. 2013;31:413–41.

9. Friese MA, Platten M, Lutz SZ, Naumann U, Aulwurm S, Bischof F, et al. MICA/NKG2D-mediated immunogene therapy of experimental gliomas. Cancer research. 2003;63:8996-9006.

10. Eisele G, Wischhusen J, Mittelbronn M, Meyermann R, Waldhauer I, Steinle A, et al. TGF-beta and metalloproteinases differentially suppress NKG2D ligand surface expression on malignant glioma cells. Brain. 2006;129:2416-25.

11. Di Tomaso T, Mazzoleni S, Wang E, Sovena G, Clavenna D, Franzin A, et al. Immunobiological characterization of cancer stem cells isolated from glioblastoma patients. Clin Cancer Res. 2010;16:800-13.

12. Wolpert F, Tritschler I, Steinle A, Weller M, Eisele G. A disintegrin and metalloproteinases 10 and 17 modulate the immunogenicity of glioblastoma-initiating cells. Neuro Oncol. 2014;16:382-91.

13. Beck BH, Kim H, O'Brien R, Jadus MR, Gillespie GY, Cloud GA, et al. Dynamics of Circulating gammadelta T Cell Activity in an Immunocompetent Mouse Model of High-Grade Glioma. PloS one. 2015;10:e0122387.

14. Bauer S, Groh V, Wu J, Steinle A, Phillips JH, Lanier LL, et al. Activation of NK cells and T cells by NKG2D, a receptor for stress-inducible MICA. Science. 1999;285:727-9.

15. Groh V, Bruhl A, El-Gabalawy H, Nelson JL, Spies T. Stimulation of T cell autoreactivity by anomalous expression of NKG2D and its MIC ligands in rheumatoid arthritis. Proceedings of the National Academy of Sciences of the United States of America. 2003;100:9452-7.

16. Sanchez-Correa B, Morgado S, Gayoso I, Bergua JM, Casado JG, Arcos MJ, et al. Human NK cells in acute myeloid leukaemia patients: analysis of NK cell-activating receptors and their ligands. Cancer immunology, immunotherapy : CII. 2011;60:1195-205.

17. Frei K, Gramatzki D, Tritschler I, Schroeder JJ, Espinoza L, Rushing EJ, et al. Transforming growth factor-beta pathway activity in glioblastoma. Oncotarget. 2015;6:5963-77.

18. Sawamura Y, Diserens AC, de Tribolet N. In vitro prostaglandin E2 production by glioblastoma cells and its effect on interleukin-2 activation of oncolytic lymphocytes. Journal of neuro-oncology. 1990;9:125-30.

19. Huettner C, Paulus W, Roggendorf W. Messenger RNA expression of the immunosuppressive cytokine IL-10 in human gliomas. The American journal of pathology. 1995;146:317-22.

20. Roth P, Junker M, Tritschler I, Mittelbronn M, Dombrowski Y, Breit SN, et al. GDF-15 contributes to proliferation and immune escape of malignant gliomas. Clin Cancer Res. 2010;16:3851-9.

21. Roth P, Mittelbronn M, Wick W, Meyermann R, Tatagiba M, Weller M. Malignant glioma cells counteract antitumor immune responses through expression of lectin-like transcript-1. Cancer Res. 2007;67:3540-4.

22. Miyazaki T, Moritake K, Yamada K, Hara N, Osago H, Shibata T, et al. Indoleamine 2,3-dioxygenase as a new target for malignant glioma therapy. Laboratory investigation. Journal of neurosurgery. 2009;111:230-7.

23. Berghoff AS, Kiesel B, Widhalm G, Rajky O, Ricken G, Wohrer A, et al. Programmed death ligand 1 expression and tumor-infiltrating lymphocytes in glioblastoma. Neuro Oncol. 2014.

24. Tran Thang NN, Derouazi M, Philippin G, Arcidiaco S, Di Berardino-Besson W, Masson F, et al. Immune infiltration of spontaneous mouse astrocytomas is dominated

643 by immunosuppressive cells from early stages of tumor development. Cancer Res.
644 2010;70:4829-39.
645
646 25. Zhou W, Ke SQ, Huang Z, Flavahan W, Fang X, Paul J, et al. Periostin secreted by
647 glioblastoma stem cells recruits M2 tumour-associated macrophages and promotes
648 malignant growth. Nat Cell Biol. 2015;17:170-82.
649
650 26. Friese MA, Wischhusen J, Wick W, Weiler M, Eisele G, Steinle A, et al. RNA
651 interference targeting transforming growth factor-beta enhances NKG2D-mediated
652 antiglioma immune response, inhibits glioma cell migration and invasiveness, and
653 abrogates tumorigenicity in vivo. Cancer Res. 2004;64:7596-603.
654
655 27. Spear P, Wu MR, Sentman ML, Sentman CL. NKG2D ligands as therapeutic
656 targets. Cancer immunity. 2013;13:8.
657
658 28. Happold C, Roth P, Wick W, Schmidt N, Florea AM, Silginer M, et al. Distinct
659 molecular mechanisms of acquired resistance to temozolomide in glioblastoma cells.
660 Journal of neurochemistry. 2012;122:444-55.
661
662 29. Hermisson M, Klumpp A, Wick W, Wischhusen J, Nagel G, Roos W, et al. O6-
663 methylguanine DNA methyltransferase and p53 status predict temozolomide sensitivity
664 in human malignant glioma cells. J Neurochem. 2006;96:766-76.
665
666 30. Maurer GD, Tritschler I, Adams B, Tabatabai G, Wick W, Stupp R, et al. Cilengitide
667 modulates attachment and viability of human glioma cells, but not sensitivity to
668 irradiation or temozolomide in vitro. Neuro Oncol. 2009;11:747-56.
669
670 31. Silginer M, Nagy S, Happold C, Schneider H, Weller M, Roth P. Autocrine activation
671 of the IFN signaling pathway may promote immune escape in glioblastoma. Neuro
672 Oncol. 2017;19:1338-49.
673
674 32. Fowler JF. The linear-quadratic formula and progress in fractionated radiotherapy.
675 Br J Radiol. 1989;62:679-94.
676
677 33. Salih HR, Antropius H, Gieseke F, Lutz SZ, Kanz L, Rammensee HG, et al.
678 Functional expression and release of ligands for the activating immunoreceptor NKG2D
679 in leukemia. Blood. 2003;102:1389-96.
680
681 34. Codo P, Weller M, Meister G, Szabo E, Steinle A, Wolter M, et al. MicroRNA-
682 mediated down-regulation of NKG2D ligands contributes to glioma immune escape.
683 Oncotarget. 2014;5:7651-62.
684
685 35. Welte SA, Sinzger C, Lutz SZ, Singh-Jasuja H, Sampaio KL, Eknigk U, et al.
686 Selective intracellular retention of virally induced NKG2D ligands by the human
687 cytomegalovirus UL16 glycoprotein. European journal of immunology. 2003;33:194-203.
688
689 36. Zafirova B, Mandaric S, Antulov R, Krmpotic A, Jonsson H, Yokoyama WM, et al.
690 Altered NK cell development and enhanced NK cell-mediated resistance to mouse
691 cytomegalovirus in NKG2D-deficient mice. Immunity. 2009;31:270-82.

37. Smyth MJ, Swann J, Kelly JM, Cretney E, Yokoyama WM, Diefenbach A, et al. NKG2D recognition and perforin effector function mediate effective cytokine immunotherapy of cancer. The Journal of experimental medicine. 2004;200:1325-35.

38. Schuffler PJ, Fuchs TJ, Ong CS, Wild PJ, Rupp NJ, Buhmann JM. TMARKER: A free software toolkit for histopathological cell counting and staining estimation. J Pathol Inform. 2013;4:S2.

39. Pohl M, Olsen KE, Holst R, Ditzel HJ, Hansen O. Tissue microarrays in non-small-cell lung cancer: reliability of immunohistochemically-determined biomarkers. Clin Lung Cancer. 2014;15:222-30 e3.

40. Hammond LA, Eckardt JR, Baker SD, Eckhardt SG, Dugan M, Forral K, et al. Phase I and pharmacokinetic study of temozolomide on a daily-for-5-days schedule in patients with advanced solid malignancies. J Clin Oncol. 1999;17:2604–13.

41. Eyler CE, Rich JN. Survival of the fittest: cancer stem cells in therapeutic resistance and angiogenesis. J Clin Oncol. 2008;26:2839-45.

42. Takada A, Yoshida S, Kajikawa M, Miyatake Y, Tomaru U, Sakai M, et al. Two novel NKG2D ligands of the mouse H60 family with differential expression patterns and binding affinities to NKG2D. Journal of immunology. 2008;180:1678-85.

43. Weller M, van den Bent M, Hopkins K, Tonn JC, Stupp R, Falini A, et al. EANO guideline for the diagnosis and treatment of anaplastic gliomas and glioblastoma. The lancet oncology. 2014;15:e395-403.

44. Lee FY, Workman P, Roberts JT, Bleehen NM. Clinical pharmacokinetics of oral CCNU (lomustine). Cancer chemotherapy and pharmacology. 1985;14:125-31.

45. Caporali S, Falcinelli S, Starace G, Russo MT, Bonmassar E, Jiricny J, et al. DNA damage induced by temozolomide signals to both ATM and ATR: role of the mismatch repair system. Molecular pharmacology. 2004;66:478-91.

46. Robertson MJ, Cochran KJ, Cameron C, Le JM, Tantravahi R, Ritz J. Characterization of a cell line, NKL, derived from an aggressive human natural killer cell leukemia. Experimental hematology. 1996;24:406-15.

47. Eriksson D, Stigbrand T. Radiation-induced cell death mechanisms. Tumour biology : the journal of the International Society for Oncodevelopmental Biology and Medicine. 2010;31:363-72.

48. Knizhnik AV, Roos WP, Nikolova T, Quiros S, Tomaszowski KH, Christmann M, et al. Survival and death strategies in glioma cells: autophagy, senescence and apoptosis triggered by a single type of temozolomide-induced DNA damage. PloS one. 2013;8:e55665.

49. Krysko O, Love Aaes T, Bachert C, Vandenabeele P, Krysko DV. Many faces of DAMPs in cancer therapy. Cell death & disease. 2013;4:e631.

50. Paolini A, Pasi F, Facoetti A, Mazzini G, Corbella F, Di Liberto R, et al. Cell death forms and HSP70 expression in U87 cells after ionizing radiation and/or chemotherapy. Anticancer research. 2011;31:3727-31.

51. Rubner Y, Muth C, Strnad A, Derer A, Sieber R, Buslei R, et al. Fractionated radiotherapy is the main stimulus for the induction of cell death and of Hsp70 release of p53 mutated glioblastoma cell lines. Radiation oncology. 2014;9:89.

52. Chitadze G, Lettau M, Luecke S, Wang T, Janssen O, Furst D, et al. NKG2D- and T-cell receptor-dependent lysis of malignant glioma cell lines by human gammadelta T cells: Modulation by temozolomide and A disintegrin and metalloproteases 10 and 17 inhibitors. Oncoimmunology. 2016;5:e1093276.

53. Cerboni C, Zingoni A, Cippitelli M, Piccoli M, Frati L, Santoni A. Antigen-activated human T lymphocytes express cell-surface NKG2D ligands via an ATM/ATR-dependent mechanism and become susceptible to autologous NK- cell lysis. Blood. 2007;110:606-15.

54. Ho SS, Gasser S. NKG2D ligands link oncogenic RAS to innate immunity. Oncoimmunology. 2013;2:e22244.

55. Wang J, Cazzato E, Ladewig E, Frattini V, Rosenbloom DI, Zairis S, et al. Clonal evolution of glioblastoma under therapy. Nat Genet. 2016;48:768-76.

56. Gasser S, Orsulic S, Brown EJ, Raulet DH. The DNA damage pathway regulates innate immune system ligands of the NKG2D receptor. Nature. 2005;436:1186-90.

57. Biddlestone-Thorpe L, Sajjad M, Rosenberg E, Beckta JM, Valerie NC, Tokarz M, et al. ATM kinase inhibition preferentially sensitizes p53-mutant glioma to ionizing radiation. Clin Cancer Res. 2013;19:3189-200.

58. Crane CA, Austgen K, Haberthur K, Hofmann C, Moyes KW, Avanesyan L, et al. Immune evasion mediated by tumor-derived lactate dehydrogenase induction of NKG2D ligands on myeloid cells in glioblastoma patients. Proceedings of the National Academy of Sciences of the United States of America. 2014;111:12823-8.

59. Ishikawa E, Tsuboi K, Saijo K, Harada H, Takano S, Nose T, et al. Autologous natural killer cell therapy for human recurrent malignant glioma. Anticancer research. 2004;24:1861-71.

Figure legends

Fig. 1. TMZ induces NKG2DL in human and mouse glioma cells including human GIC independent from cell death and growth inhibition. A LN-18 or LN-229 glioma cells were exposed to different concentrations of TMZ or DMSO control. Viability was assessed by live/dead staining at 72 h (black dotted line), cytostatic effects were detected by crystal violet staining at 72 h and 20 d (grey dashed and straight lines) (left panels). Transcripts for MICA, MICB, ULBP2 or ULBP3 were assessed by real-time PCR after 48 h (middle panels). Data represent mean values ± SD from 3 independent experiments (*$p < 0.05$; **$p < 0.01$). NKG2DL protein levels at the cell surface were determined by flow cytometry following exposure to TMZ or DMSO control for 72 h (right panels). Data are presented as SFI and mean values ± SD from 3 independent experiments are shown (*$p < 0.05$; **$p < 0.01$). Grey areas represent TMZ plasma levels achieved in patients. B, C. S-24 or ZH-305 glioma-initiating cell lines (B) and GL-261 or SMA-560 mouse glioma cells (C) were treated as indicated and human or murine NKG2DL were analysed as in (A).

Fig. 2. IR induces NKG2DL in human and mouse glioma cells independent from cell death and cell growth inhibition. A. LN-18 or LN-229 glioma cells were irradiated with different doses of gamma irradiation. Viability was assessed by live/dead staining (black dotted line), cytostatic effects were detected by crystal violet staining (grey dashed and straight lines) (left panels). Transcripts (MICA, MICB, ULBP2 or ULBP3) were assessed by real-time PCR after 48 h (middle). Data represent mean values ± SD from independent experiments (*$p < 0.05$; **$p < 0.01$). NKG2DL protein levels at the cell

surface were determined by flow cytometry 72 h after IR (right). Data are presented as SFI and mean values ± SD from 3 independent experiments are shown (*p < 0.05; **p < 0.01). B, C. S-24 or ZH-305 glioma-initiating cell lines (B) and GL-261 or SMA-560 mouse glioma cells (C) were irradiated as indicated and human or mouse NKG2DL were assessed as in (A).

Fig. 3. NKG2DL induction is modulated by MGMT and depends on ATM. A. Whole cell lysates of LN-18_control or LN18_shMGMT cells and LN-229_control or LN-229_MGMT were assessed by immunoblot for MGMT protein levels. Beta-actin was used as a control. Acute cytostatic and clonogenic effects after exposure to TMZ were determined by crystal violet staining at the indicated time points. B. The cells were exposed to TMZ and cell surface expression of MICA and MICB was determined after 72 h by flow cytometry. Data are presented as SFI and mean +/- SD of 3 independent experiments is shown (*p < 0.05; **p < 0.01). C. LN-229 (left) or S-24 (right) cells were treated with KU-60019 or DMSO 4 h prior to TMZ exposure. Immunofluorescence images were acquired following $pATM^{Ser1981}$ staining (red). Nuclei are stained with DAPI (blue). D. LN-229 (left) or S-24 (right) were exposed to TMZ (upper row) or IR (lower panel) after ATM inhibition using KU-60019 or siRNA-mediated gene silencing. MICA and MICB cell surface expression were determined by flow cytometry. Data are presented as SFI and mean values ± SD from 2 independent experiments are shown (*p < 0.05; **p < 0.01).

Fig. 4. Exposure to TMZ or IR promotes glioma cell immunogenicity in a NKG2D-dependent manner. A. Upper panel: LN-229 (left) or S-24 (right) cells, pre-exposed to TMZ (grey line) or DMSO control (black line) for 48 h, were used as target cells in a 3 h immune cell lysis assays using polyclonal NK (for LN-229) or NKL (for S-24) effector cells at various effector : target (E:T) ratios. Following TMZ treatment, viable glioma cells were counted before co-incubation with effector cells and immune-mediated cytolysis was corrected for spontaneous background lysis. Lower panel: NKL cells were pre-incubated with anti-NKG2D antibody or isotype control and subsequently used as effector cells in lysis assays with LN-229 or S-24 glioma cells, either pre-exposed to TMZ or DMSO control, at an E:T ratio of 20:1. B. LN-229 or S-24 cells were irradiated with 2 Gy prior to use as target cells in 3 h lysis assays. The experimental setup was the same as in (A). In all figures mean +/- SD of triplicates from 1 representative out of 2 independent experiments is shown (*$p < 0.05$; **$p < 0.01$).

Fig. 5. TMZ and IR induce NKG2DL *in vivo* in syngeneic glioma models and human glioblastoma patients have increased tumor-associated NKG2DL after radiochemotherapy. A. Orthotopic tumor-bearing mice (SMA-560_TurboFP in VM/Dk mice (left) or GL-261_niRP in C57BL/6 mice (right)) received a single dose of local irradiation (12 Gy) on day 10 or TMZ (10 mg/kg/day) per oral gavage from day 7-11 after tumor implantation. Mice were sacrificed on day 12, tumors were dissociated and cells analyzed for NKG2DL cell surface expression by flow cytometry. Tumor cells were gated in the dot plot diagrams based on the fluorescent signal. Histograms represent mean fluorescence intensity of RAE-1, MULT-1 and

H60 on these cells. The diagrams summarize results of 5 mice per group. Data are presented as mean fluorescence intensity ± SD (*p < 0.05; **p < 0.01). B. NKG2DL were assessed on mRNA (upper panel) and surface protein level (lower panel) in matched pairs of human primary and recurrent tumors. Positive cell surface staining events were quantified in an unsupervised fashion with the TMARKER toolkit. (*p < 0.05; ns = non-significant).

Fig. 6. The NKG2D system contributes to the therapeutic effects of TMZ and IR in glioma. A. SMA-560 tumor-bearing mice received injections of anti-NKG2D or isotype control antibody one day before and one day and then every 7 days after tumor implantation. Subsequently, the animals were treated with TMZ or solvent control from day 7-11 or a single dose of IR at day 12. Survival data are presented as Kaplan-Meier plots (left and center). Combined analysis of median survival is plotted on the right. Survival differences were compared between different treatment groups (*p < 0.05; **p < 0.01) and within a treatment group between isotype or anti-NKG2D treatment (+p < 0.05; ++p < 0.01). B-D. GL-261 tumor-bearing C57BL/6 or NKG2D$^{-/-}$ mice were treated with IR (single local dose of 12 Gy at day 10), TMZ (10 mg/kg p.o., day 7-11) or the combination of both. B. Survival data are presented as Kaplan-Meier plots (left and center). Combined analysis of median survival of the different groups is plotted on the right (*p < 0.05; **p < 0.01 between treatment groups and +p < 0.05; ++p < 0.01 within a treatment group for intact NKG2D vs. NKG2D$^{-/-}$). C. T2-weigthed coronal scans were acquired at day 13 after tumor implantation. Two representative scans for each group are shown (left). The white arrow marks the tumor region. Mean +/- SD of

the tumor volume in mm^3 from 4 mice/group is shown (right). D. Percentage of NK, CD4, CD8, and $\gamma\delta$ T cells (left) and the corresponding IFN-γ secretion (right) of tumor-infiltrating lymphocytes derived from mice described in B and C were determined at day 14 after tumor implantation. Mean +/- SD from 3 mice is shown (*$p < 0.05$; **$p < 0.01$ between treatment groups and +$p < 0.05$; ++$p < 0.01$ within a treatment group for intact NKG2D vs. $NKG2D^{-/-}$).

Fig. 1

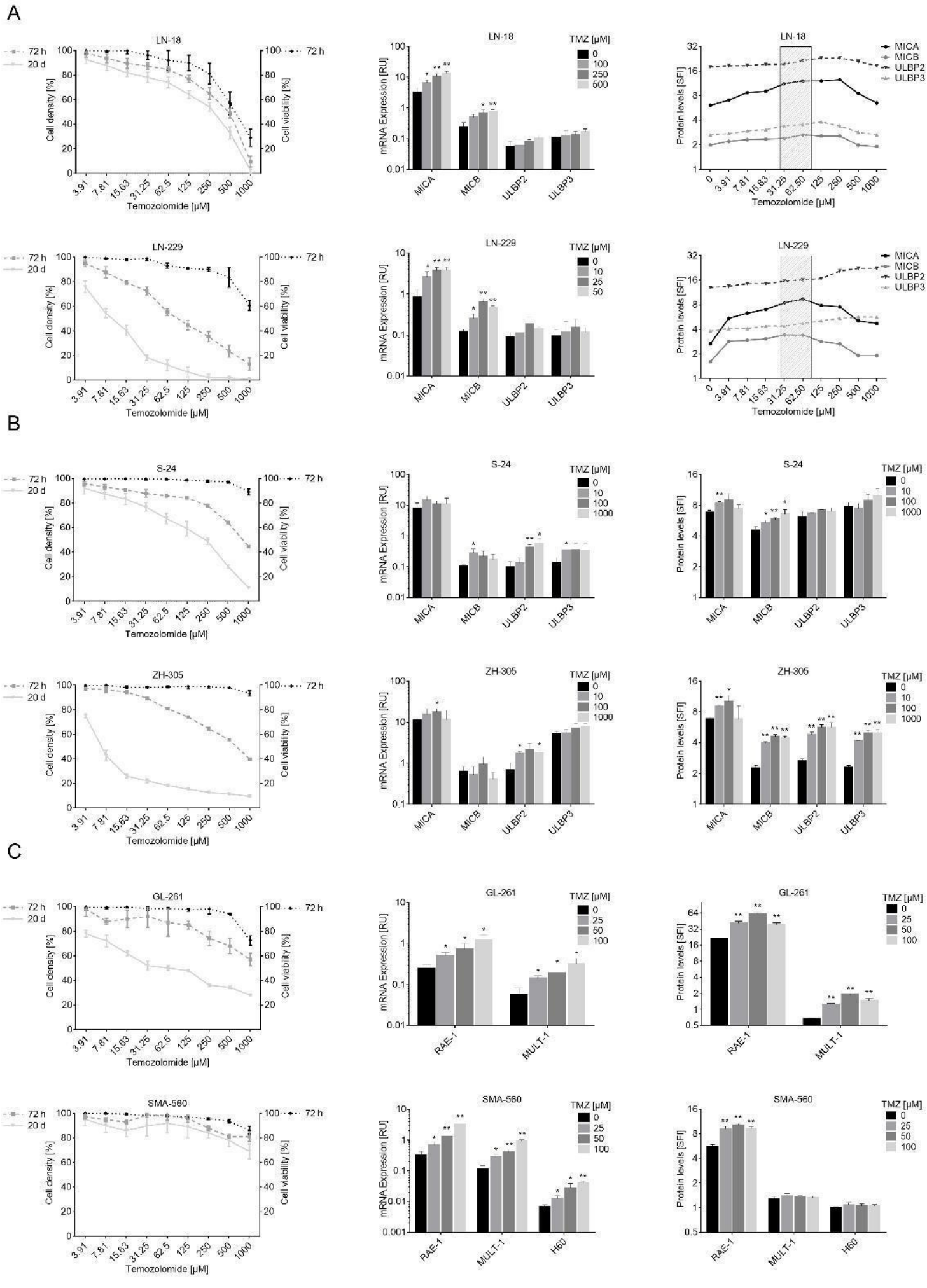
A
LN-18
72 h
20 d
Cell density [%]
Cell viability [%]
Temozolomide [µM]
mRNA Expression [RU]
TMZ [µM]
0
100
250
500
MICA
MICB
ULBP2
ULBP3
Protein levels [SFI]
LN-229
10
25
50
B
S-24
1000
ZH-305
C
GL-261
RAE-1
MULT-1
SMA-560
H60

Fig. 2

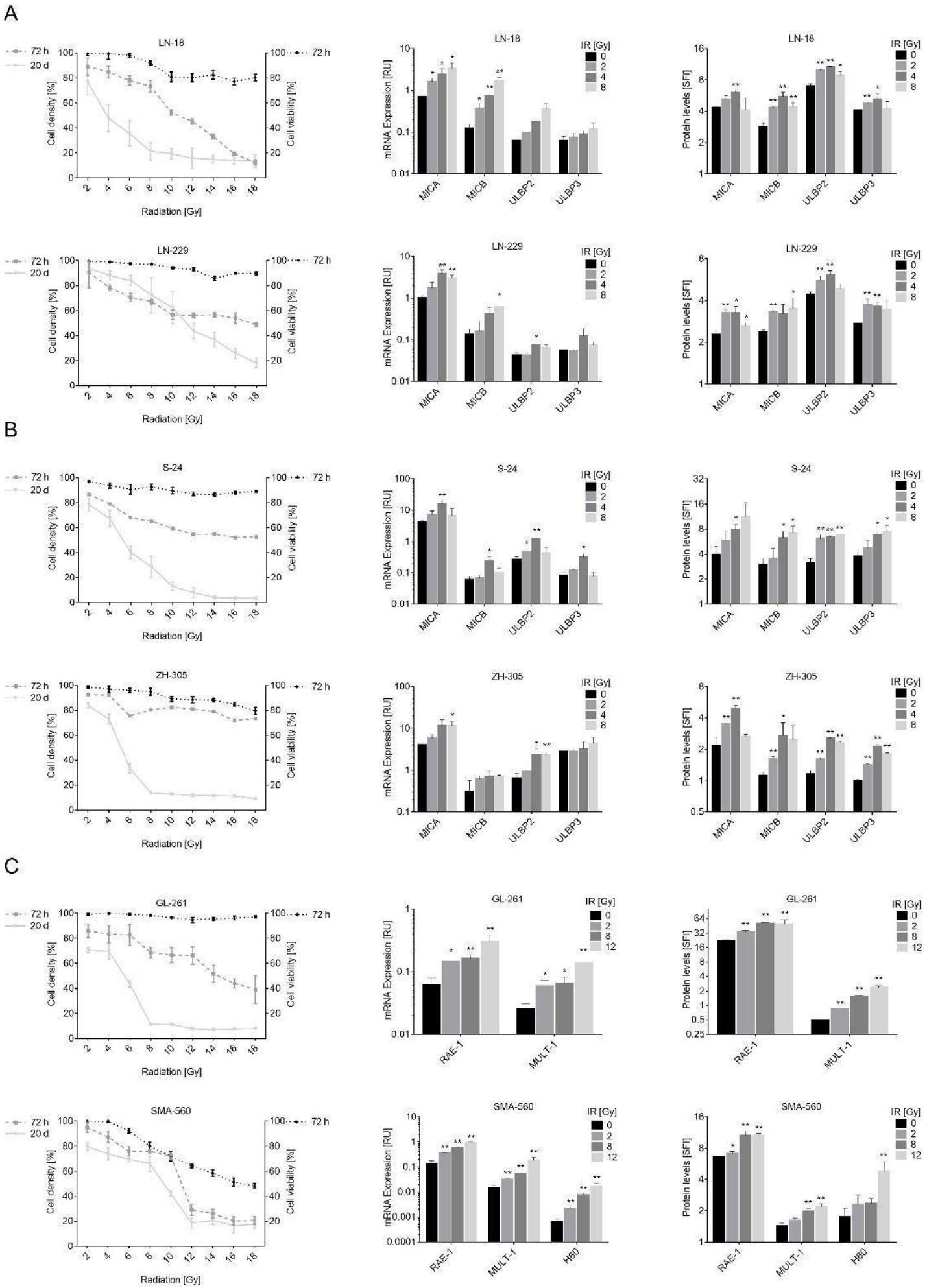
A
LN-18
72 h
20 d
Cell density [%]
Cell viability [%]
Radiation [Gy]
mRNA Expression [RU]
Protein levels [SFI]
IR [Gy]
0
2
4
8
MICA
MICB
ULBP2
ULBP3
LN-229
B
S-24
ZH-305
C
GL-261
12
RAE-1
MULT-1
SMA-560
H60

Fig. 3

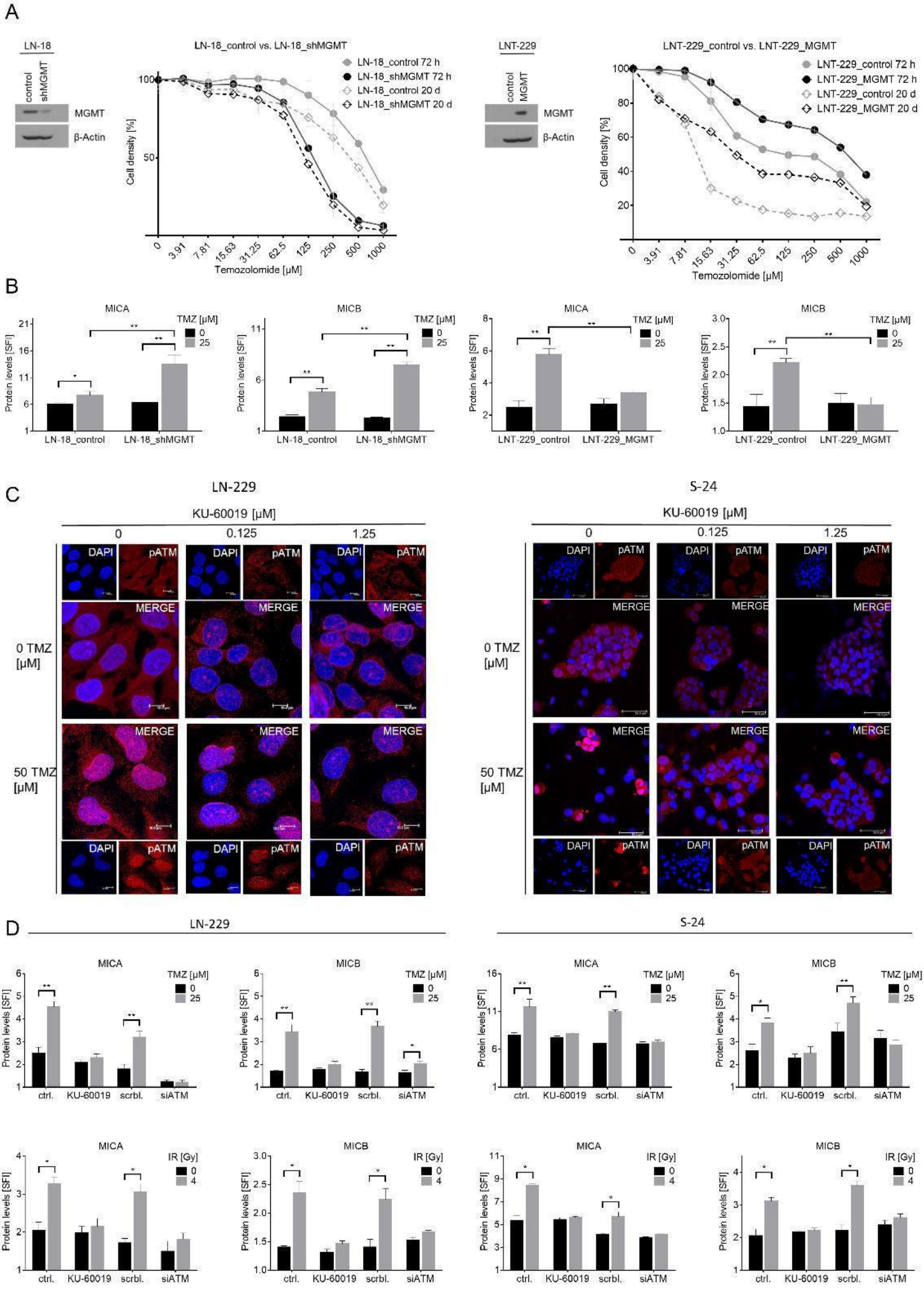
A
LN-18
control
shMGMT
MGMT
β-Actin
LN-18_control vs. LN-18_shMGMT
LN-18_control 72 h
LN-18_shMGMT 72 h
LN-18_control 20 d
LN-18_shMGMT 20 d
Cell density [%]
Temozolomide [µM]
LNT-229
control
MGMT
MGMT
β-Actin
LNT-229_control vs. LNT-229_MGMT
LNT-229_control 72 h
LNT-229_MGMT 72 h
LNT-229_control 20 d
LNT-229_MGMT 20 d
Cell density [%]
Temozolomide [µM]
B
MICA
MICB
TMZ [µM]
0
25
Protein levels [SFI]
LN-18_control
LN-18_shMGMT
LNT-229_control
LNT-229_MGMT
C
LN-229
S-24
KU-60019 [µM]
0
0.125
1.25
DAPI
pATM
MERGE
0 TMZ [µM]
50 TMZ [µM]
D
LN-229
S-24
MICA
MICB
TMZ [µM]
IR [Gy]
0
4
25
Protein levels [SFI]
ctrl.
KU-60019
scrbl.
siATM

Fig. 4

A

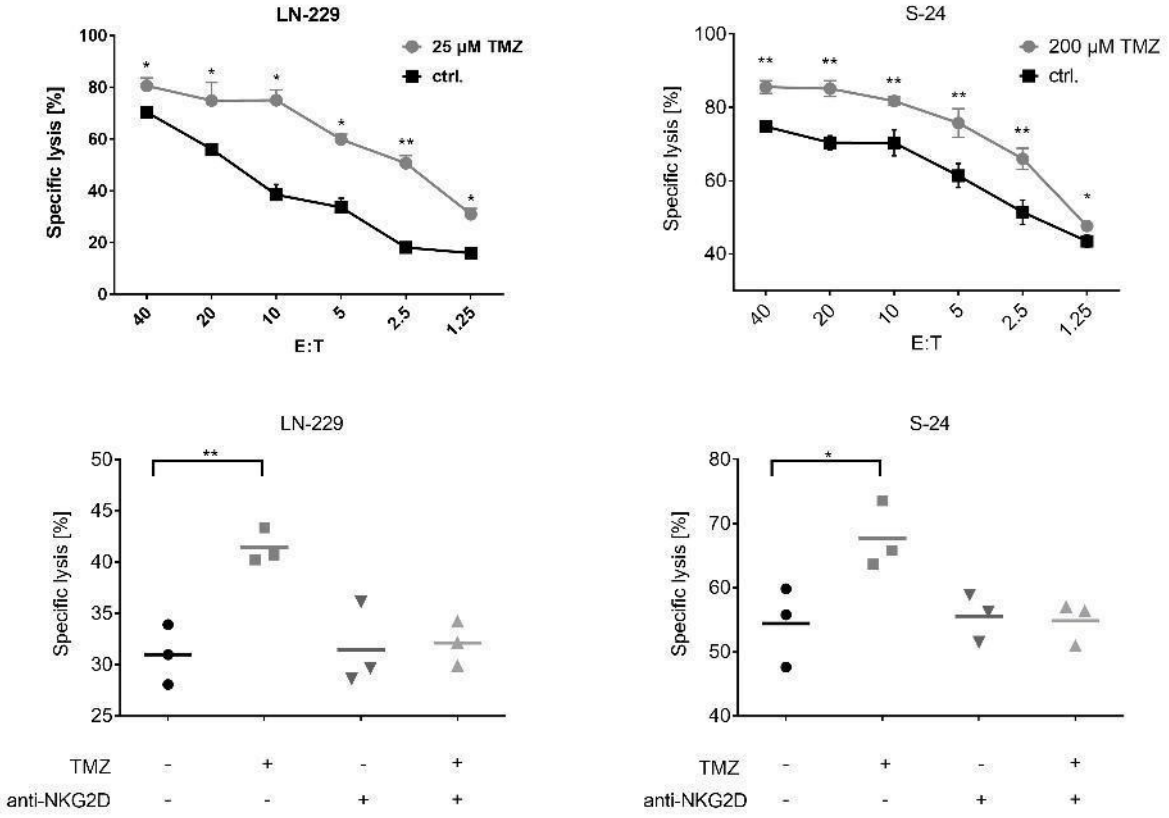
LN-229
25 µM TMZ
ctrl.
Specific lysis [%]
E:T
S-24
200 µM TMZ
ctrl.
Specific lysis [%]
E:T
LN-229
Specific lysis [%]
TMZ
anti-NKG2D
S-24
Specific lysis [%]
TMZ
anti-NKG2D

B

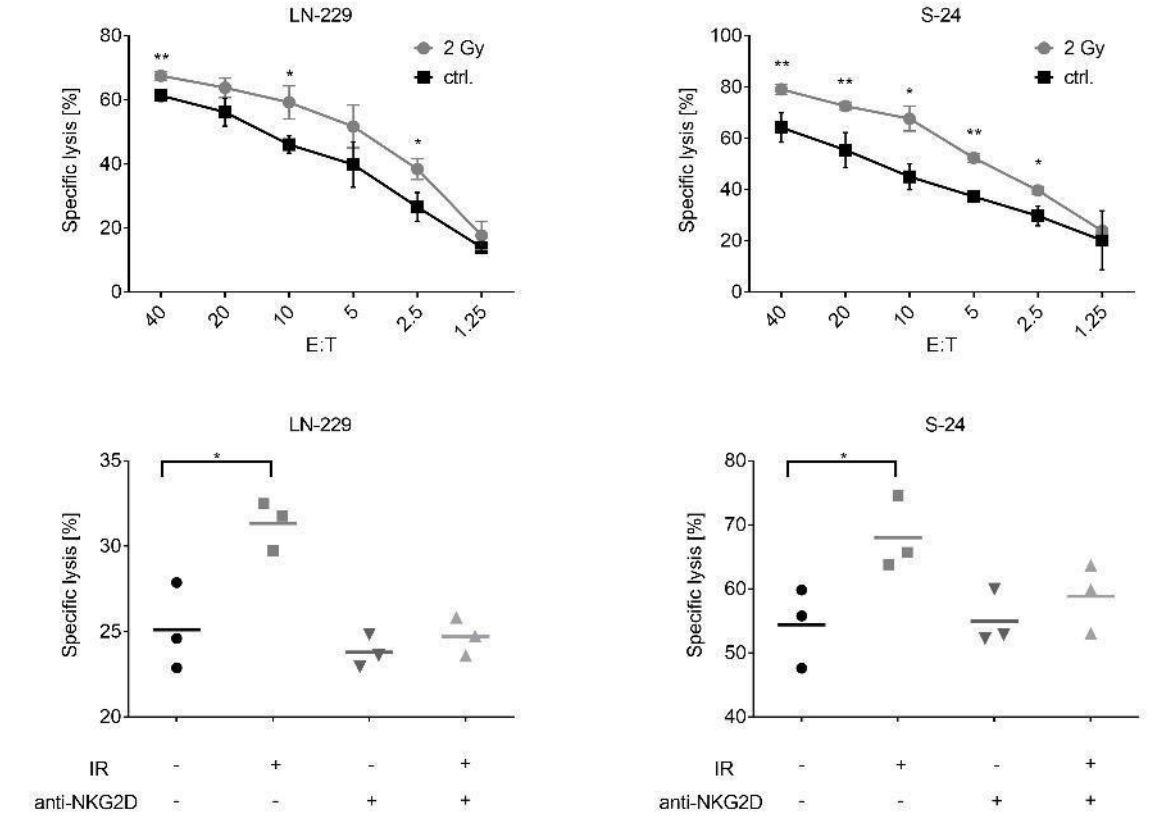
LN-229
2 Gy
ctrl.
Specific lysis [%]
E:T
S-24
2 Gy
ctrl.
Specific lysis [%]
E:T
LN-229
Specific lysis [%]
IR
anti-NKG2D
S-24
Specific lysis [%]
IR
anti-NKG2D

Fig. 5

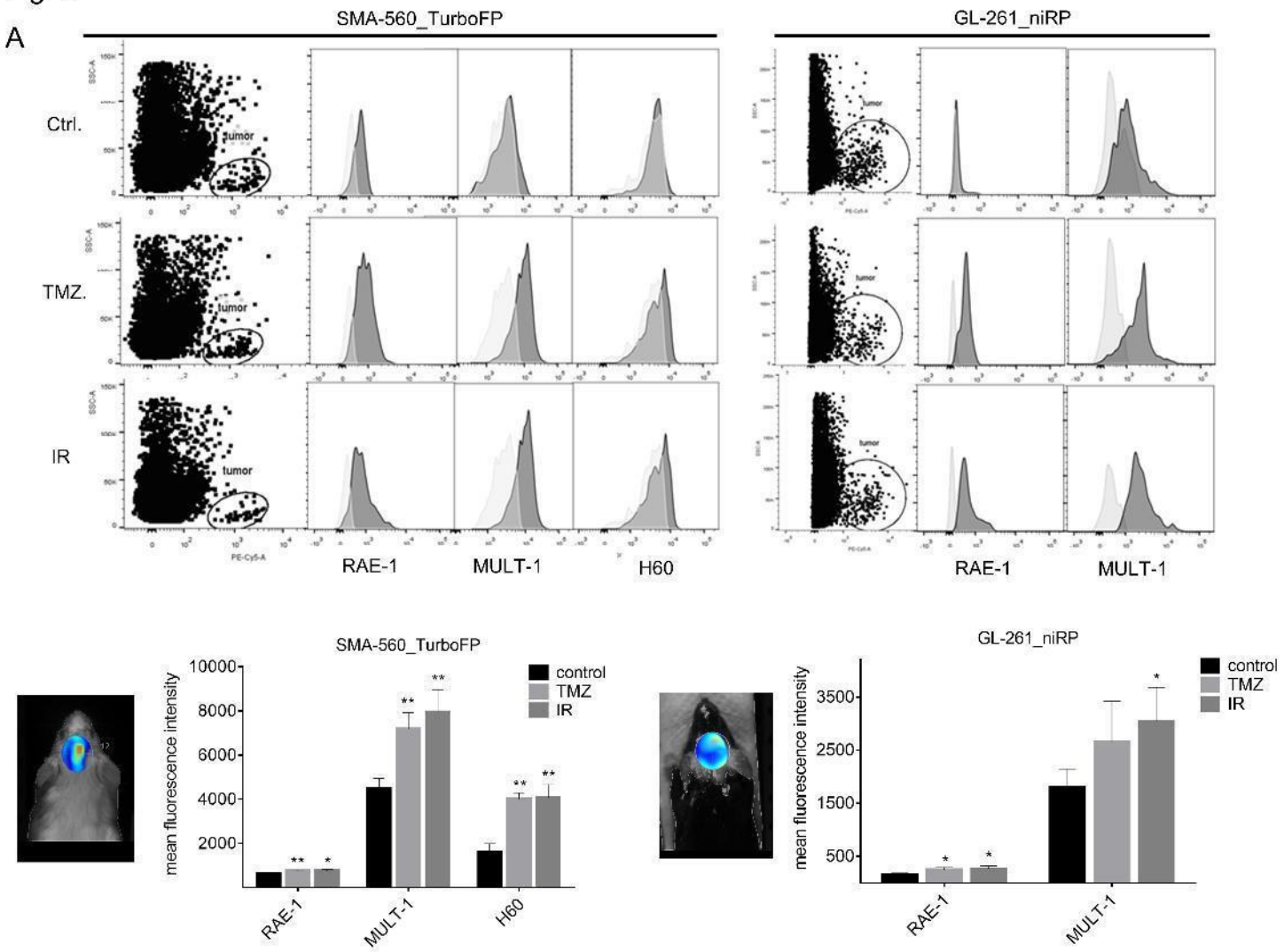
A
SMA-560_TurboFP
GL-261_niRP
Ctrl.
TMZ.
IR
tumor
RAE-1
MULT-1
H60
SMA-560_TurboFP
GL-261_niRP
control
TMZ
IR
mean fluorescence intensity
RAE-1
MULT-1
H60

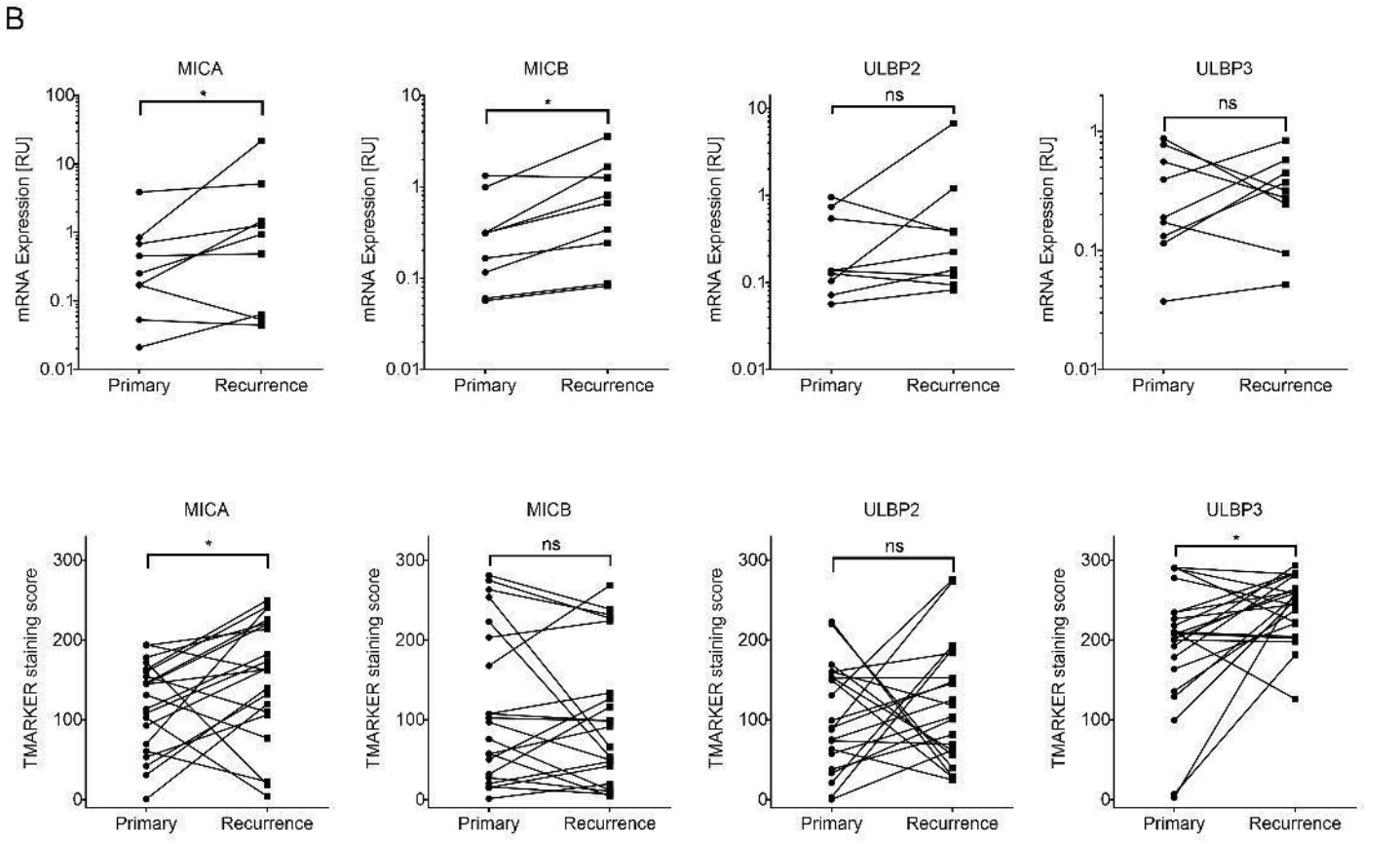
B
MICA
MICB
ULBP2
ULBP3
mRNA Expression [RU]
TMARKER staining score
Primary
Recurrence
ns

Fig. 6

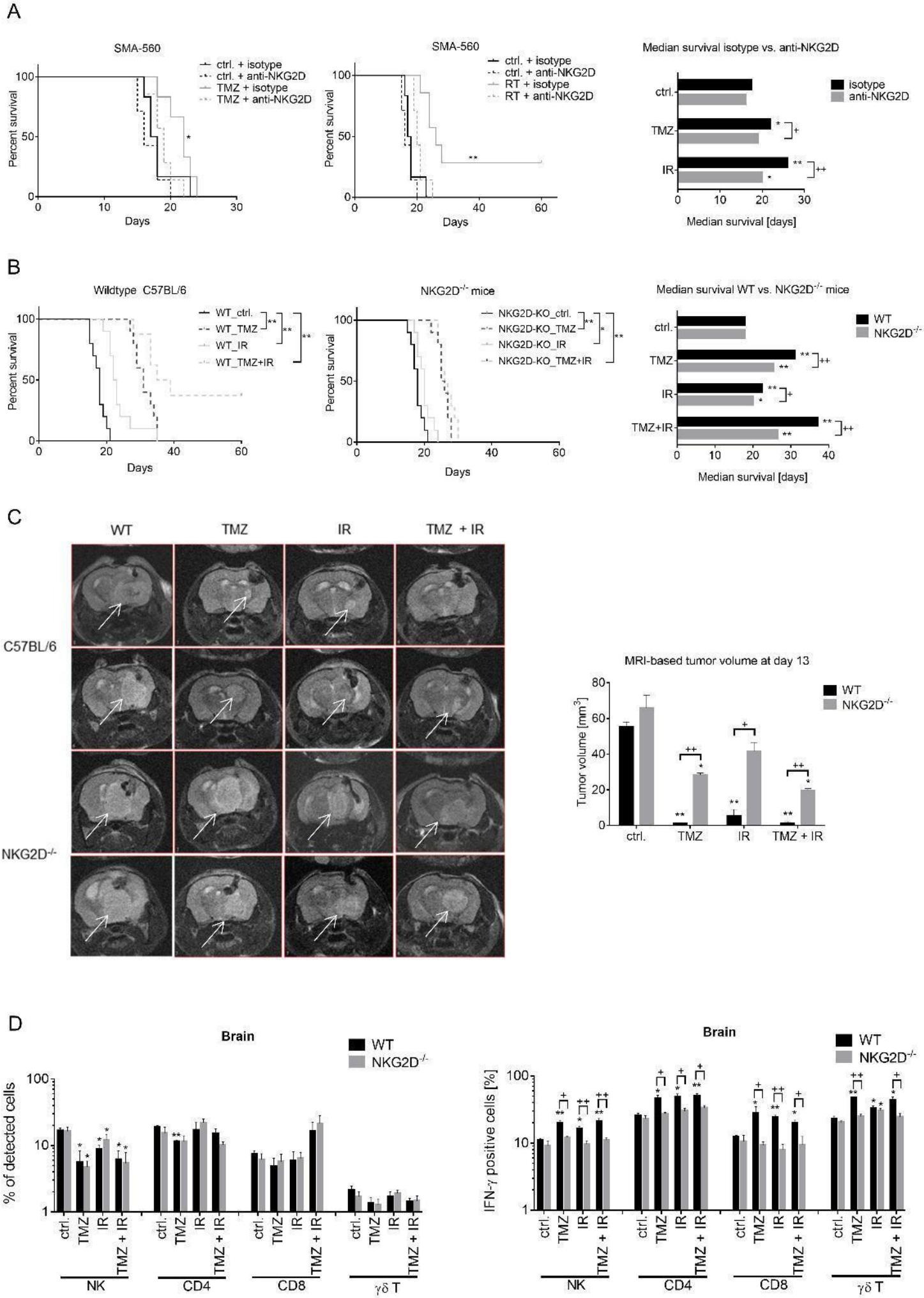
A
SMA-560
ctrl. + isotype
ctrl. + anti-NKG2D
TMZ + isotype
TMZ + anti-NKG2D
Percent survival
Days
SMA-560
ctrl. + isotype
ctrl. + anti-NKG2D
RT + isotype
RT + anti-NKG2D
Median survival isotype vs. anti-NKG2D
isotype
anti-NKG2D
ctrl.
TMZ
IR
Median survival [days]
B
Wildtype C57BL/6
WT_ctrl.
WT_TMZ
WT_IR
WT_TMZ+IR
NKG2D-/- mice
NKG2D-KO_ctrl.
NKG2D-KO_TMZ
NKG2D-KO_IR
NKG2D-KO_TMZ+IR
Median survival WT vs. NKG2D-/- mice
WT
NKG2D-/-
TMZ+IR
C
WT
TMZ
IR
TMZ + IR
C57BL/6
NKG2D-/-
MRI-based tumor volume at day 13
Tumor volume [mm3]
D
Brain
% of detected cells
IFN-γ positive cells [%]
NK
CD4
CD8
γδ T

Supplementary Materials:

Supplementary figure 1

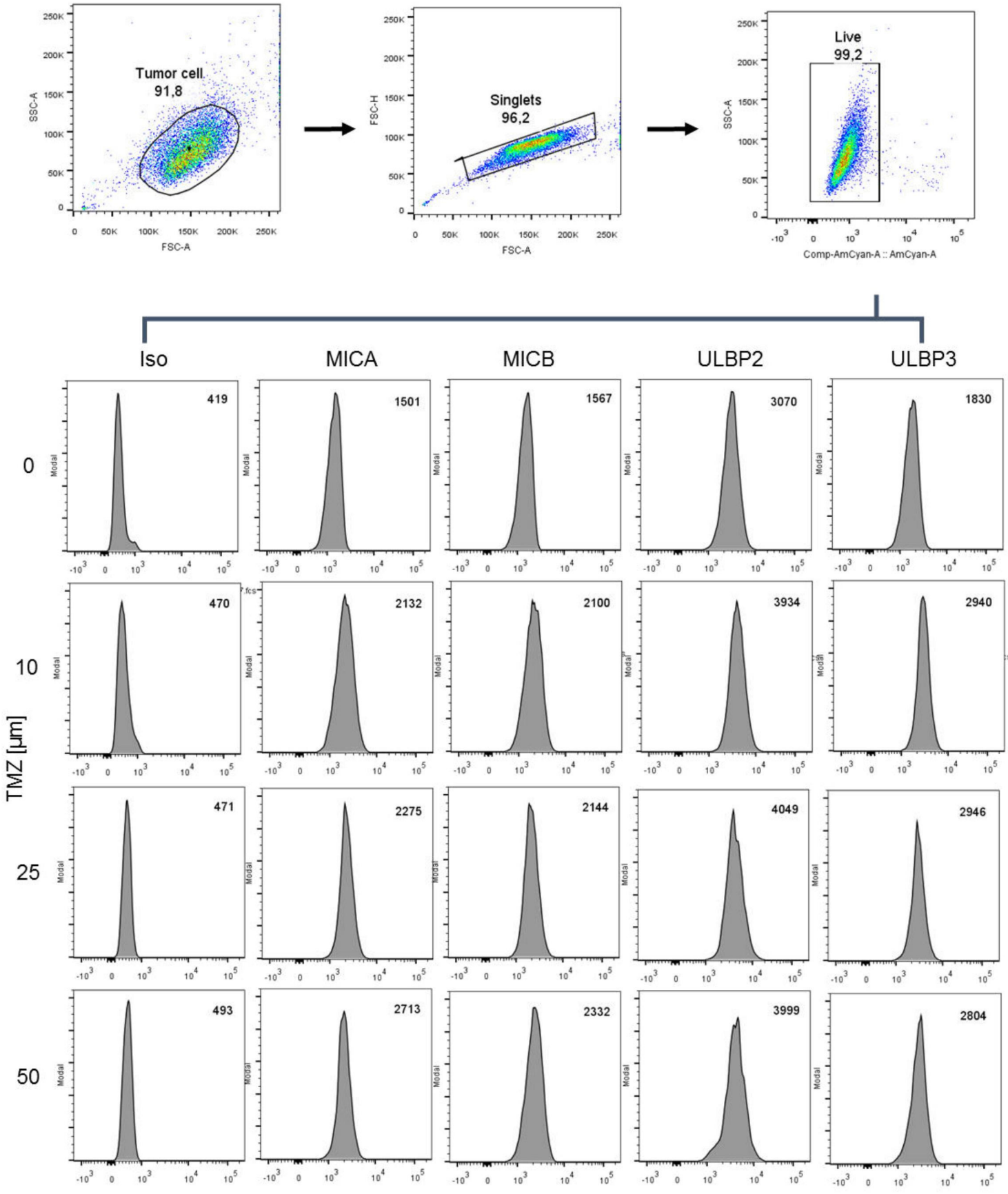

Suppl. Fig. 1. Gating strategy for detection of cell surface NKG2DL.

Representative data for LN-229 cells 72 h after treatment with different concentrations of TMZ is shown. Within the tumor cell population, we gated on single living cells. Cell surface expression after staining with isotype control, anti-MICA, anti-MICB, anti-ULPB2, or anti-ULBP3 are displayed in histograms. Numbers in the upper right corners indicate the mean fluorescence intensity, which allows further calculation of specific fluorescence indexes (SFI) by dividing median fluorescence obtained with the specific antibody by median fluorescence obtained with isotype control antibody.

Supplementary figure 2

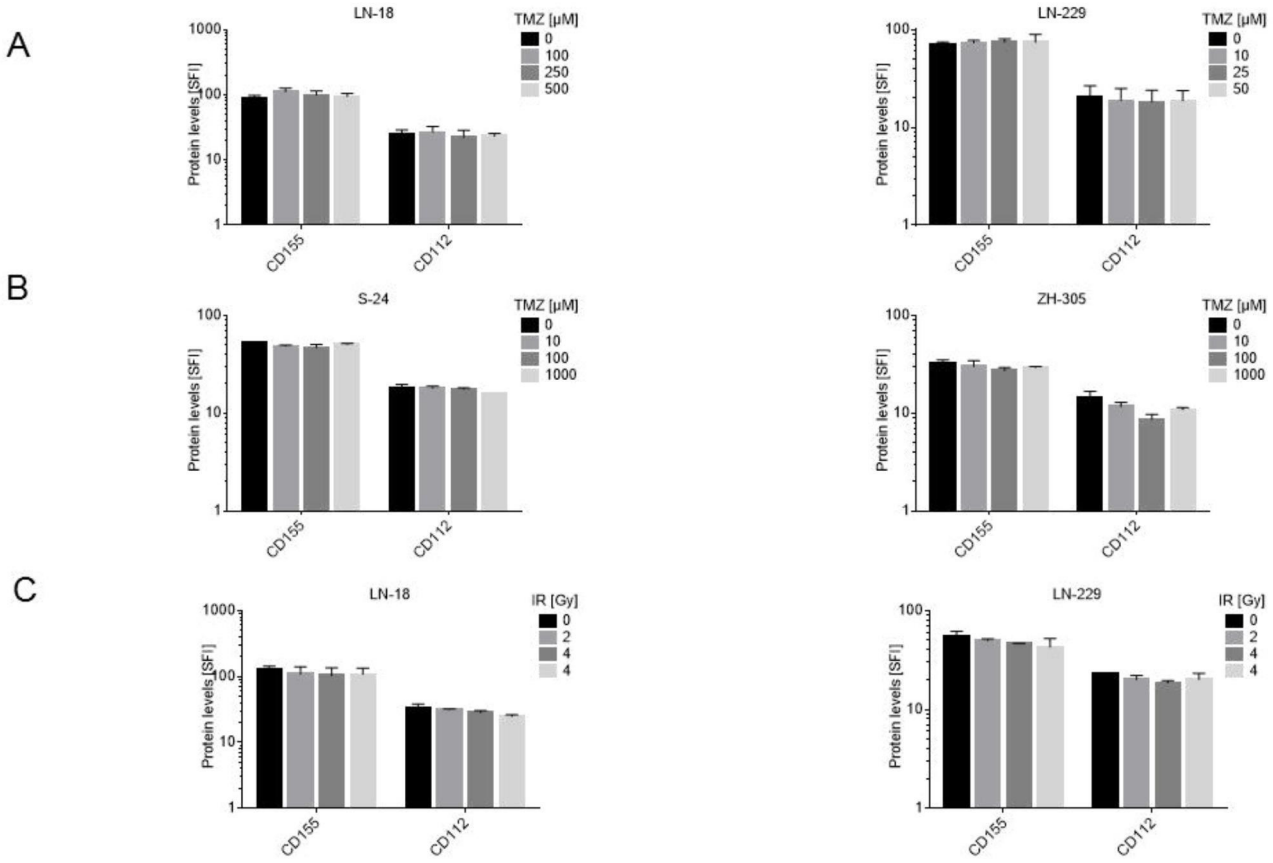

Suppl. Fig. 2. DNAM-1 ligands are not induced upon treatment of TMZ or IR. CD112 and CD155 protein levels at the cell surface of LN-18 or LN-229 cells (A) or S-24 or ZH-305 (B) were determined by flow cytometry 72 h after exposure to TMZ or DMSO or single irradiation of LN-18 or LN-229 cells (C). Data are shown as SFI and median+/- SD from 3 independent experiments is shown.

Supplementary figure 3

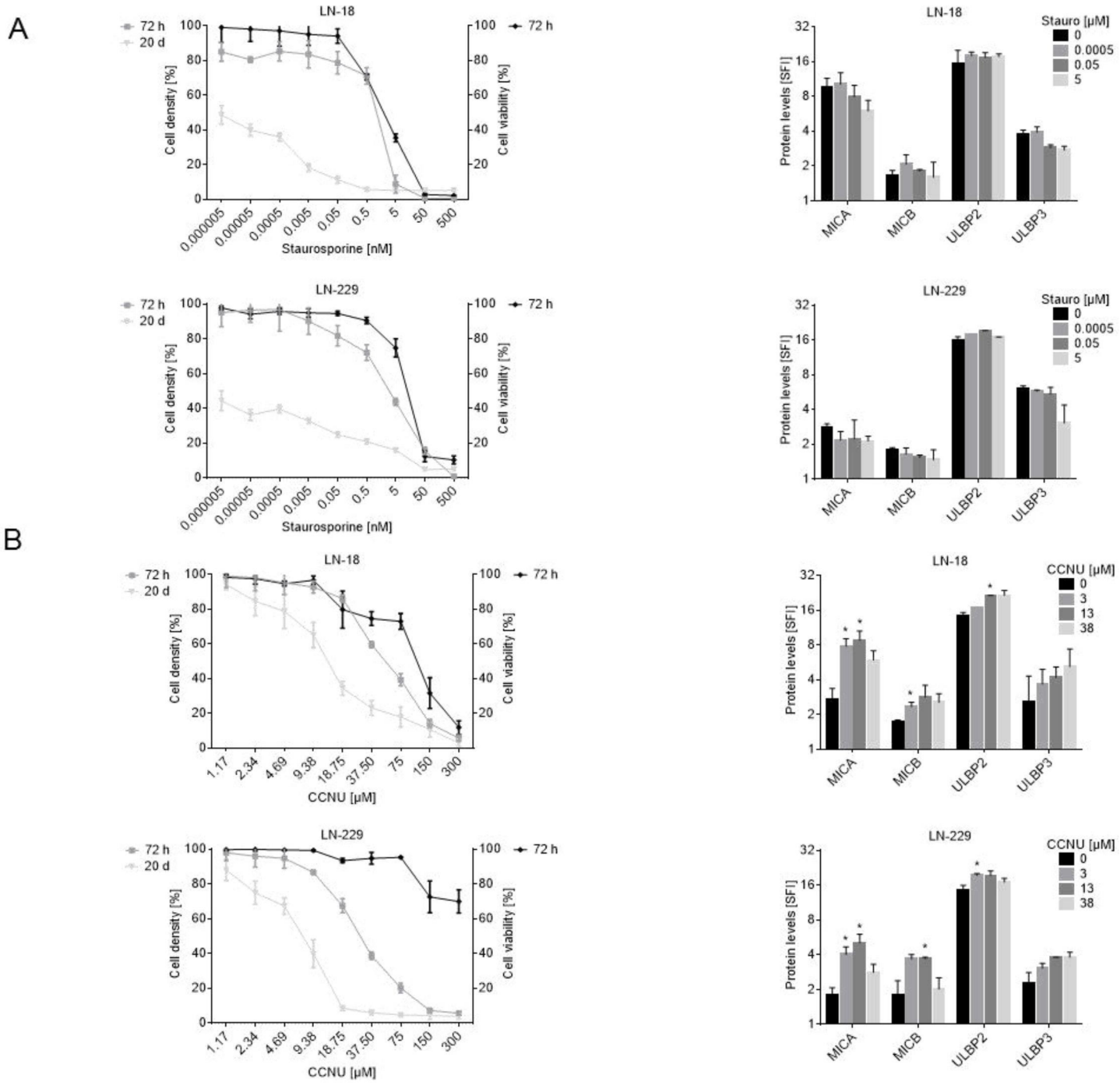

Suppl. Fig. 3. Induction of NKG2DL is not an unspecific response to cell death induction in glioma cells. A. LN-18 (upper panel) or LN-229 (lower panel) cells were exposed to different concentrations of staurosporine. Viability was assessed by live/dead staining at 72 h (black line), cytostatic effects were detected by crystal violet staining at 72 h and 20 d (grey lines) (left panels). NKG2DL protein levels at the cell surface were determined by flow cytometry following exposure to staurosporine or DMSO control for 72 h (right panels). Data are presented as SFI and mean values ± SD from 2 independent experiments are shown (*p < 0.05; **p < 0.01). B. Same experimental setup as in A, but the cells were exposed to different concentrations of CCNU.

Supplementary figure 4

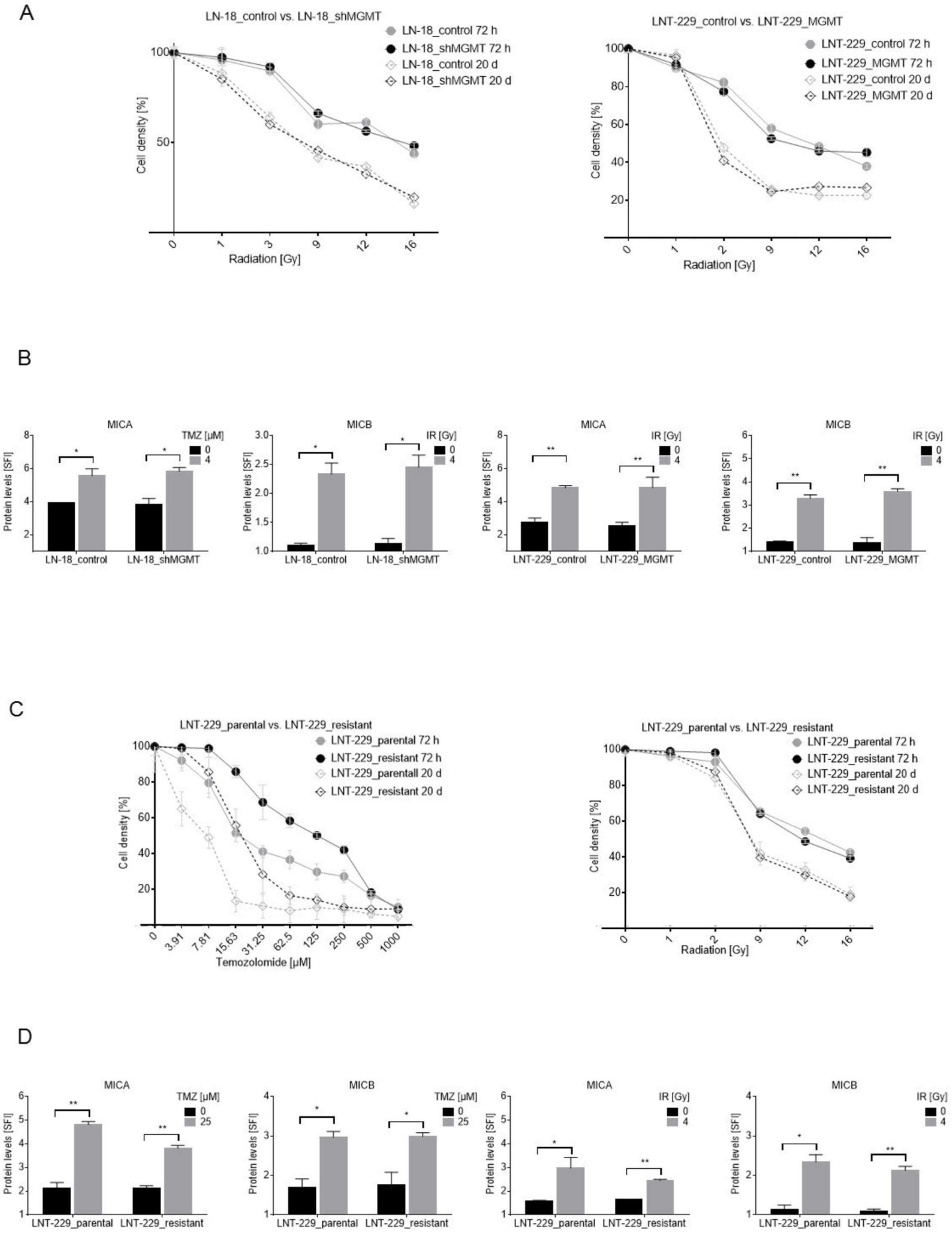

Suppl. Fig. 4. MGMT does not affect irradiation-induced NKG2DL expression and NKG2DL can be induced in glioma cells with acquired TMZ resistance A. LN-18_shMGMT and the corresponding LN-18_control cells or LN-229_MGMT and the corresponding LN-229_control cells were irradiated with increasing doses. Cell density was assessed by crystal violet staining after 72 h (acute cytostatic effect) or 20 days (clonogenic cell survival), respectively. B. On the cells described in A, cell surface expression of MICA and MICB was determined after 72 h by flow cytometry. Data are presented as SFI and mean values ± SD from 2 independent experiments are shown (*$p < 0.05$; **$p < 0.01$). C. LNT-229 cells with acquired resistance to TMZ or parental control cells were exposed to different concentrations of TMZ (upper panel, left graph) or doses of irradiation (upper panel, right graph). Cytostatic effects were detected by crystal violet staining at 72 h and 20 d. D. On the cells described in C, NKG2DL protein levels at the cell surface were determined by flow cytometry 72 h after exposure to TMZ (left graph) or irradiation (right graph). Data are presented as SFI and mean values ± SD from 2 independent experiments are shown (*$p < 0.05$; **$p < 0.01$).

Supplementary figure 5

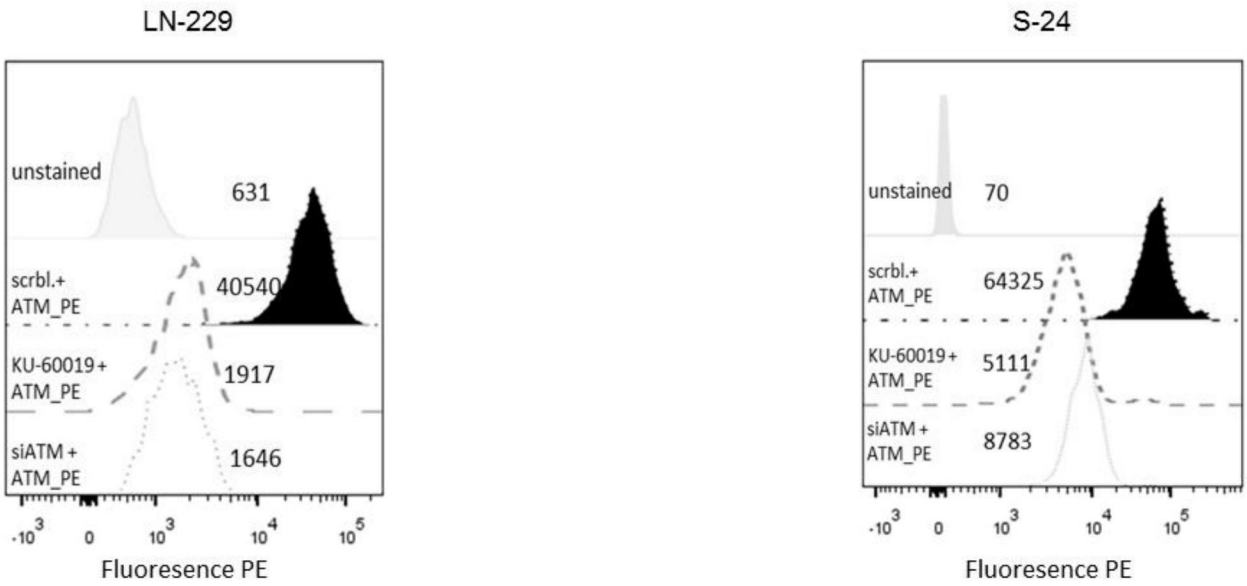

Suppl. Fig. 5. Inhibition of ATM in LN-229 or S-24 cells. LN-229 or S-24 cells were exposed to 1.25 µM of KU-60019 or siRNA oligonucleotides specific for ATM or scrambled control. After 72 h, the cells were stained with anti-phospho-ATM^{Ser1981} PE antibody and assessed by flow cytometry. Data are presented as mean fluorescence intensity (indicated by numbers).

Supplementary figure 6

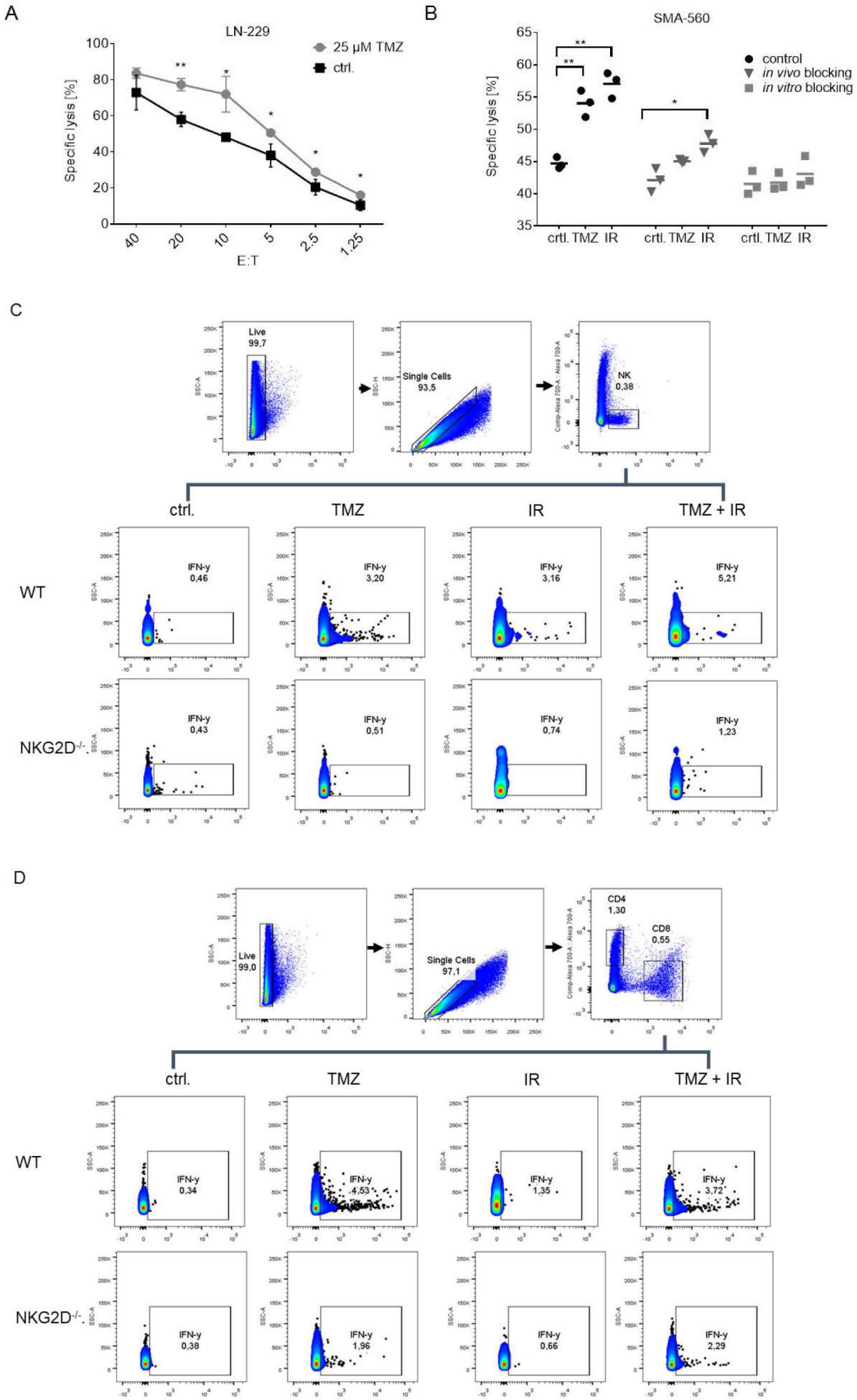

Suppl. Fig. 6. Functional consequences of NKG2DL induction by TMZ or IR. A. Exposure to TMZ promotes immune-cell mediated glioma cell lysis. LN-229 cells, pre-exposed to TMZ (grey line) or DMSO control (black line) for 48 h, were used as target cells in a 3 h lysis assays using NKL effector cells at various effector : target (E:T) ratios. B. Blocking of NKG2D signaling with an inhibitory antibody *in vivo.* SMA-560 tumor-bearing mice that were treated with vehicle ctrl. (day 7-11), TMZ (day 7-11) or local IR (10 Gy at day 10) and received injections of anti-NKG2D or isotype control antibody one day before and every 7 days after tumor implantation. At day 14, splenocytes from these mice were used as effector cells in immune cell lysis assays. Target cells were SMA-560 cells pre-treated *in vitro* with TMZ, RT or not. E:T was 20:1. As an additional control, splenocytes from non tumor-bearing, untreated mice were pre-treated *ex vivo* with blocking anti-NKG2D antibody and used as effector cells against the described target cells. C and D. Gating strategy for detection of tumor-infiltrating NK, CD4 and CD8 T cells. Fourteen days after tumor implantation, tumor-infiltrating lymphocytes were isolated after tumor dissociation and Percoll separation. $NKp46^{+}CD3^{-}$ cells were determined as percentage of NK cells (C). Numbers indicate the percentage of positive cells. Furthermore, CD4 and CD8 positive cells were gated (D). Plots are representative for one out of three mice.